

國立交通大學

應用數學系

碩士論文

有界面 Stokes 方程之邊界積分方法

Boundary integral method for Stokes flow with interfaces



研究生：吳聲華

指導教授：賴明治 教授

中華民國一百年六月

有界面 Stokes 方程之邊界積分方法

Boundary integral method for Stokes flow with interfaces

研究生：吳聲華

Student : Sheng - Hua Wu

指導教授：賴明治

Advisor : Ming - Chih Lai

國立交通大學
應用數學系
碩士論文



Submitted to Department of Applied Mathematics

College of Science

National Chiao Tung University

in partial Fulfillment of the Requirements

for the Degree of

Master

in

Applied Mathematics

June 2011

Hsinchu, Taiwan, Republic of China

中華民國一百年六月

有界面 Stokes 方程之邊界積分方法

學生：吳聲華

指導教授：賴明治

國立交通大學應用數學學系（研究所）碩士班



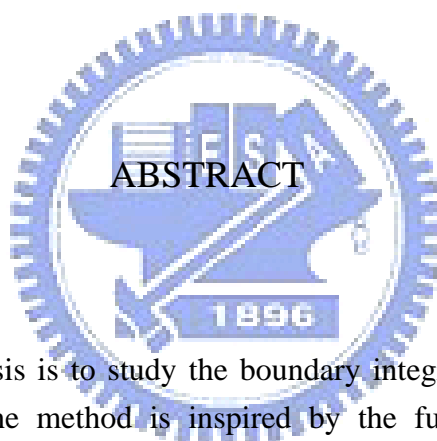
本文主要的目的是研究二維不可壓縮 Stokes 方程的邊界積分方法。此數值方法是基於 Poisson 方程的基本解，和將界面速度表示為 Green 函數與奇異來源項之捲積。我們分析積分方程的奇異性以及將積分方程分解成為平滑部分和奇異部分。前者可以利用梯形法作積分計算，後者則利用 quadrature 形式來計算。兩個數值計算格式被提出用來模擬彈性界面的動態，一個是顯式的計算格式，另一個是隱式的計算格式。在數值實驗中，我們首先模擬橢圓彈性界面在靜止流體的動態，得到一個二階收斂的結果。第二個數值實驗是模擬單一 vesicle 在剪流中的動態，得到一系列與理論相對照的數值結果。

Boundary integral method for Stokes flow with interfaces

Student : Sheng-Hua Wu

Advisors : Ming-Chih Lai

Department (Institute) of Applied Mathematics
National Chiao Tung University



The essential purpose of this thesis is to study the boundary integral method for two dimensional incompressible Stokes flows. The method is inspired by the fundamental solution of Poisson equation, and presents the interfacial velocity in integral formulae, as convolution form of a Green's function and a singular source term. Once the formulae are clear, we analyze the singularity in the integral equations and split it into a smooth part and a singular part. The former can be treated by the trapezoidal rule and the later is cured by quadrature form with specific weights. To simulate the dynamics of an elastic interface, two numerical schemes are proposed, one is the explicit scheme which a force in previous time step is equipped, the other is implicit so that a tension-like unknown is solved together with interfacial velocity. In numerical experiments, we first apply the method to an elliptic elastic material in a quiescent flow, and give a second-order convergence to the circular steady state. The second application is a vesicle suspended in a simple shear flow. A series of numerical studies about the tank-treading motion and the tumbling motion for a vesicle match previous works well.

誌 謝

本篇論文的完成，首先要感謝我的指導教授 — 賴明治老師。在老師的細心指點之下，讓我一點一滴熟悉數值偏微分方程以及科學計算的方法。我也從自己的研究中找到對數值偏微分方程以及科學計算這塊領域的興趣與成就感。除了指導教授外，在我們科學計算研究室中的其他學長們也給了我很多的幫助。感謝黃仲尹學長、曾昱豪學長、馮可安學長、陳冠羽學長以及胡偉帆學長無私的分享他們的知識與經驗，讓此篇論文可以順利完成。

在論文口試期間，承蒙吳金典教授與楊肅煜教授費心審閱並提供許多寶貴意見，使得本論文變得更加完備，學生永遠銘記在心。

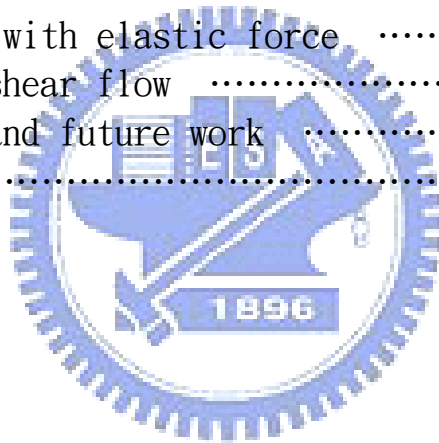


平常除了做數值計算研究外，我也要感謝同屆的碩士班同學們，他們和我分享彼此的興趣，讓我的研究生生活多采多姿，處處充滿著樂趣。

最後，我要好好地感謝我的家人，是他們鼓勵並支持著我做研究的興趣，讓我可以無所顧忌地完成我的學業。希望能與他們，以及在我身邊所有關心我的人，一起分享這篇論文完成的喜悅與榮耀。

目 錄

中文提要	i
英文提要	ii
誌謝	iii
目錄	iv
一、	Introduction	1
二、	Derivation of boundary integral equation	2
2.1	Green's function for two dimensional Stokes flow	3
2.2	Boundary integral equation	5
2.3	Interfacial flow	7
三、	Numerical method	9
3.1	Explicit numerical integration schemes	10
3.2	Implicit numerical integration schemes	14
四、	Numerical results	19
4.1	Stokes flow with elastic force	19
4.2	Vesicle in shear flow	22
五、	Conclusion and future work	28
Reference	29



1 Introduction

Stokes flow involving interfaces have been researched extensively in the past few years. It has many important applications in science and engineering, such as in biomechanics, geophysics, mechanical engineering, and chemical engineering. One example is the flow of a suspension of bubbles, drops or biological cells, such as a red blood cell past through a vessel. Numerical simulations can accurately approach the practical questions when analytical solutions cannot be found and real experiments are hard to realize or expensive to execute. While numerical simulations become a very important tool for investigating the interfacial dynamics in low Reynolds number flow, studying surface tension on interface is popular. Surface tension effects are modelled classically by positing a force jump at the interface. There are many numerical methods that are suitable for computing interfacial dynamics in Stokes flow, including boundary integral methods [8, 9, 10, 11, 13], level set methods, immersed interface methods [6], immersed boundary methods [4], phase-field and diffused interface methods. Each method has its merits and disadvantages. In this thesis, we focus on the boundary integral method to simulate the interfacial dynamics in two dimensional incompressible Stokes flow. The three dimensional problem is more challenging to study especially for evolving interfaces with large deformations. In this thesis, we study the boundary integral method for two dimensional incompressible Stokes flow. The method is inspired by the fundamental solution of Poisson equation, and presents the interfacial velocity in integral formulae, as convolution form of a Green's function and a singular source term. Once the formulae are clear, we analyze the singularity in the integral equations and split it into a smooth part and a singular part. The former can be treated by the trapezoidal rule and the later is cured by quadrature form with specific weights. To simulate the dynamics of an elastic interface, two numerical schemes are proposed, one is the explicit scheme which a force in previous time step is equipped, the other is implicit so that a tension-like unknown is solved together with interfacial velocity. In numerical experiments, we first apply the method to an elliptic elastic material in a quiescent flow, and give a second-order convergence to the circular steady state. The second application is a vesicle suspended in a simple shear flow. A series of numerical studies about the tank-treading motion and the tumbling motion for a vesicle match previous works well.

Organization of this thesis is as follows. In Section 2, we introduce the Green's function for the two dimensional incompressible Stokes flow, and derive the boundary integral equation for the two dimensional incompressible Stokes flow. The derivation is based on Pozrikidis' book [7]. In Section 3, we discuss the boundary integral equation for the interfacial velocity in detail by decomposing the integrals into different terms, and present the explicit and the implicit numerical integration schemes for different situations. This introduction is based on Xu Sun and Xiaofan Li's paper [11]. In Section 4, we present some numerical experiments for simulating the interfacial dynamics in Stokes flow with the elastic and the motion of a vesicle suspended in a simple shear flow. Moreover, we present the convergence test for the velocity to verify the accuracy of the numerical inte-

gration schemes.

2 Derivation of boundary integral equation

First of all, let us consider the flow governed by the two dimensional Navier-Stokes equation with the condition of incompressibility

$$\rho \left(\frac{\partial \mathbf{u}}{\partial t} + \mathbf{u} \cdot \nabla \mathbf{u} \right) = -\nabla P + \mu \Delta \mathbf{u}, \quad (2.1)$$

$$\nabla \cdot \mathbf{u} = 0, \quad (2.2)$$

where $\mathbf{u} = (u, v)$, ρ is the density of the fluid, and μ is the viscosity of the fluid. In order to nondimensionalize the Navier-Stokes equation, we introduce a characteristic length L , a characteristic velocity U , and a characteristic time T . Moreover, let $\mathbf{x}^* = \frac{\mathbf{x}}{L}$, $\mathbf{u}^* = \frac{\mathbf{u}}{U}$, $t^* = \frac{tU}{L}$, and $P^* = \frac{PL}{\mu U}$. Then, the Navier-Stokes equation can be rewritten in the dimensionless form

$$\beta \frac{\partial \mathbf{u}^*}{\partial t^*} + Re \mathbf{u}^* \cdot \nabla^* \mathbf{u}^* = -\nabla^* P^* + \Delta^* \mathbf{u}^*. \quad (2.3)$$

There are two dimensionless numbers in (2.3): the frequency parameter $\beta = \frac{L^2}{\nu T}$ and the Reynolds number $Re = \frac{UL}{\nu}$, where $\nu = \frac{\mu}{\rho}$ is the kinematic viscosity of fluid. The frequency parameter β represents the ratio between the inertial acceleration force and the viscous force, and the Reynolds number Re represents the ratio between the inertial force and the viscous force. When β and Re are much smaller than 1, all terms on the left hand side of (2.3) are much smaller than the terms on the right hand side. Thus, all terms on the left hand side of (2.3) can be ignored. Then reverting to dimensional variables, we can find that the Navier-Stokes equation becomes the Stokes equation

$$-\nabla P + \mu \Delta \mathbf{u} = \nabla \cdot \boldsymbol{\sigma} = 0, \quad (2.4)$$

where $\boldsymbol{\sigma}$ is the stress tensor defined as

$$\boldsymbol{\sigma} = \begin{bmatrix} \sigma_{11} & \sigma_{12} \\ \sigma_{21} & \sigma_{22} \end{bmatrix} = \begin{bmatrix} -P + 2\mu \left(\frac{\partial u}{\partial x} \right) & \mu \left(\frac{\partial u}{\partial y} + \frac{\partial v}{\partial x} \right) \\ \mu \left(\frac{\partial u}{\partial y} + \frac{\partial v}{\partial x} \right) & -P + 2\mu \left(\frac{\partial v}{\partial y} \right) \end{bmatrix}. \quad (2.5)$$

Taking the divergence of the Stokes equation and using the condition of incompressibility, we find that the pressure is a harmonic function

$$\Delta P = 0. \quad (2.6)$$

2.1 Green's function for two dimensional Stokes flow

The following description is based on Pozrikidis' book [7]. Now consider the two dimensional incompressible singular force Stokes equation

$$-\nabla P + \mu \Delta \mathbf{u} + \mathbf{g} \delta(\mathbf{X} - \mathbf{X}_0) = 0, \quad (2.7)$$

$$\nabla \cdot \mathbf{u} = 0,$$

where $\mathbf{g} = (g_1, g_2)$ is an arbitrary constant, δ is the delta function, and $\mathbf{X}_0 = (X_0, Y_0)$ is an arbitrary point. Introducing the Green's function for the singular force Stokes equation

$$\mathbf{G}(\mathbf{X}, \mathbf{X}_0) = \begin{bmatrix} G_{11}(\mathbf{X}, \mathbf{X}_0) & G_{12}(\mathbf{X}, \mathbf{X}_0) \\ G_{21}(\mathbf{X}, \mathbf{X}_0) & G_{22}(\mathbf{X}, \mathbf{X}_0) \end{bmatrix},$$

such that the velocity $\mathbf{u}(\mathbf{X})$ can be expressed as

$$\mathbf{u}(\mathbf{X}) = \begin{bmatrix} u(\mathbf{X}) \\ v(\mathbf{X}) \end{bmatrix} = \frac{1}{4\pi\mu} \begin{bmatrix} G_{11}(\mathbf{X}, \mathbf{X}_0)g_1 + G_{12}(\mathbf{X}, \mathbf{X}_0)g_2 \\ G_{21}(\mathbf{X}, \mathbf{X}_0)g_1 + G_{22}(\mathbf{X}, \mathbf{X}_0)g_2 \end{bmatrix}, \quad (2.8)$$

where \mathbf{X}_0 is called the source point, and \mathbf{X} is called the observation point. Physically, (2.8) expresses the velocity field due to a point force of strength \mathbf{g} located at the point \mathbf{X}_0 . Since the pressure $P(\mathbf{X})$ is a harmonic function, then there exists a function $\mathbf{p}(\mathbf{X}, \mathbf{X}_0) = (p_1(\mathbf{X}, \mathbf{X}_0), p_2(\mathbf{X}, \mathbf{X}_0))$ such that $P(\mathbf{X}) = \frac{1}{4\pi}(p_1(\mathbf{X}, \mathbf{X}_0)g_1 + p_2(\mathbf{X}, \mathbf{X}_0)g_2)$. Once we get the velocity $\mathbf{u}(\mathbf{X})$ and the pressure $P(\mathbf{X})$, then we can obtain the stress tensor $\boldsymbol{\sigma}(\mathbf{X})$ by substituting the velocity and the pressure into (2.5).

We compute the free space Green's function as following. First, we replace the delta function in (2.7) with the fundamental solution of the Laplace equation

$$\delta(\hat{\mathbf{X}}) = \frac{1}{2\pi} \Delta \ln r, \quad (2.9)$$

where $\hat{\mathbf{X}} = (\hat{X}, \hat{Y}) = \mathbf{X} - \mathbf{X}_0$, and $r = \|\hat{\mathbf{X}}\|$. Substituting (2.9) into (2.7), we have

$$-\nabla P + \mu \Delta \mathbf{u} + \left(\frac{1}{2\pi} \Delta \ln r \right) \mathbf{g} = 0.$$

Taking the divergence for above equation, we have

$$-\Delta P + \nabla \cdot \left[\left(\frac{1}{2\pi} \Delta \ln r \right) \mathbf{g} \right] = 0 \Rightarrow \Delta P = \Delta \left[\left(\frac{1}{2\pi} \nabla \ln r \right) \cdot \mathbf{g} \right]. \quad (2.10)$$

Thus, we can obtain the pressure P by balancing the dimension of (2.10)

$$P = \left(\frac{1}{2\pi} \nabla \ln r \right) \cdot \mathbf{g}. \quad (2.11)$$

Next, substituting (2.9) and (2.11) into (2.7), we have

$$\begin{aligned} & -\nabla \left[\left(\frac{1}{2\pi} \nabla \ln r \right) \cdot \mathbf{g} \right] + \mu \Delta \mathbf{u} + \left(\frac{1}{2\pi} \Delta \ln r \right) \mathbf{g} = 0 \\ \Rightarrow \mu \Delta \mathbf{u} &= \begin{bmatrix} -\frac{\partial^2}{\partial y^2} \left(\frac{1}{2\pi} \ln r \right) & \frac{\partial^2}{\partial x \partial y} \left(\frac{1}{2\pi} \ln r \right) \\ \frac{\partial^2}{\partial x \partial y} \left(\frac{1}{2\pi} \ln r \right) & -\frac{\partial^2}{\partial x^2} \left(\frac{1}{2\pi} \ln r \right) \end{bmatrix} \mathbf{g}. \end{aligned} \quad (2.12)$$

Assume that the velocity \mathbf{u} can be expressed as

$$\mathbf{u} = \frac{1}{\mu} \begin{bmatrix} -\frac{\partial^2}{\partial y^2} H & \frac{\partial^2}{\partial x \partial y} H \\ \frac{\partial^2}{\partial x \partial y} H & -\frac{\partial^2}{\partial x^2} H \end{bmatrix} \mathbf{g}, \quad (2.13)$$

where H is a scalar function. It is noted that the condition of incompressibility $\nabla \cdot \mathbf{u} = 0$ is satisfied under this assumption. Substituting (2.13) into (2.12), we have

$$\Delta \left\{ \begin{bmatrix} -\frac{\partial^2}{\partial y^2} H & \frac{\partial^2}{\partial x \partial y} H \\ \frac{\partial^2}{\partial x \partial y} H & -\frac{\partial^2}{\partial x^2} H \end{bmatrix} \mathbf{g} \right\} = \begin{bmatrix} -\frac{\partial^2}{\partial y^2} \left(\frac{1}{2\pi} \ln r \right) & \frac{\partial^2}{\partial x \partial y} \left(\frac{1}{2\pi} \ln r \right) \\ \frac{\partial^2}{\partial x \partial y} \left(\frac{1}{2\pi} \ln r \right) & -\frac{\partial^2}{\partial x^2} \left(\frac{1}{2\pi} \ln r \right) \end{bmatrix} \mathbf{g}.$$

Since the constant vector \mathbf{g} is arbitrary, then

$$\Delta H = \frac{1}{2\pi} \ln r.$$

We can obtain the scalar function H by solving above equation

$$H = \frac{1}{8\pi} r^2 (\ln r - 1).$$

Finally, we can obtain the velocity \mathbf{u} by substituting H into (2.13)

$$\mathbf{u}(\mathbf{X}) = \begin{bmatrix} u(\mathbf{X}) \\ v(\mathbf{X}) \end{bmatrix} = \frac{1}{4\pi\mu} \begin{bmatrix} G_{11}(\mathbf{X}, \mathbf{X}_0) & G_{12}(\mathbf{X}, \mathbf{X}_0) \\ G_{21}(\mathbf{X}, \mathbf{X}_0) & G_{22}(\mathbf{X}, \mathbf{X}_0) \end{bmatrix} \mathbf{g},$$

where $\mathbf{G}(\mathbf{X}, \mathbf{X}_0)$ is the free space Green's function

$$\mathbf{G}(\mathbf{X}, \mathbf{X}_0) = \begin{bmatrix} -\ln r + \frac{\hat{X}^2}{r^2} & \frac{\hat{X}\hat{Y}}{r^2} \\ \frac{\hat{X}\hat{Y}}{r^2} & -\ln r + \frac{\hat{Y}^2}{r^2} \end{bmatrix}.$$

The associated pressure P and the stress tensor $\boldsymbol{\sigma}$ can be computed as following

$$\begin{aligned} P(\mathbf{X}) &= \frac{1}{2\pi} \left(\frac{\hat{X}g_1}{r^2} + \frac{\hat{Y}g_2}{r^2} \right), \\ \boldsymbol{\sigma}(\mathbf{X}) &= \frac{-1}{\pi} \begin{bmatrix} \frac{\hat{X}^3 g_1}{r^4} + \frac{\hat{X}^2 \hat{Y} g_2}{r^4} & \frac{\hat{X}^2 \hat{Y} g_1}{r^4} + \frac{\hat{X} \hat{Y}^2 g_2}{r^4} \\ \frac{\hat{X}^2 \hat{Y} g_1}{r^4} + \frac{\hat{X} \hat{Y}^2 g_2}{r^4} & \frac{\hat{X} \hat{Y}^2 g_1}{r^4} + \frac{\hat{Y}^3 g_2}{r^4} \end{bmatrix}. \end{aligned}$$

2.2 Boundary integral equation

Once the free space Green's function is obtained, we can derive the boundary integral equation by the Lorentz reciprocal identity, which is for any two nonsingular flows \mathbf{u} and \mathbf{u}' with corresponding stress tensors $\boldsymbol{\sigma}$ and $\boldsymbol{\sigma}'$

$$\nabla \cdot (\boldsymbol{\sigma}\mathbf{u}' - \boldsymbol{\sigma}'\mathbf{u}) = 0 \Rightarrow \nabla \cdot \left(\begin{bmatrix} \sigma_{11} & \sigma_{12} \\ \sigma_{21} & \sigma_{22} \end{bmatrix} \begin{bmatrix} u' \\ v' \end{bmatrix} - \begin{bmatrix} \sigma'_{11} & \sigma'_{12} \\ \sigma'_{21} & \sigma'_{22} \end{bmatrix} \begin{bmatrix} u \\ v \end{bmatrix} \right) = 0 \quad (2.14)$$

Now let \mathbf{u}' be the solution of the two dimensional singular force Stokes equation and $\boldsymbol{\sigma}'$ be the corresponding stress tensors. Substituting these expressions into the Lorentz reciprocal identity, we have

$$\nabla \cdot \left(\begin{bmatrix} \sigma_{11} & \sigma_{12} \\ \sigma_{21} & \sigma_{22} \end{bmatrix} \begin{bmatrix} G_{11}g_1 + G_{12}g_2 \\ G_{21}g_1 + G_{22}g_2 \end{bmatrix} - 4\mu \begin{bmatrix} \frac{\hat{X}^3g_1}{r^4} + \frac{\hat{X}^2\hat{Y}g_2}{r^4} & \frac{\hat{X}^2\hat{Y}g_1}{r^4} + \frac{\hat{X}\hat{Y}^2g_2}{r^4} \\ \frac{\hat{X}^2\hat{Y}g_1}{r^4} + \frac{\hat{X}\hat{Y}^2g_2}{r^4} & \frac{\hat{X}\hat{Y}^2g_1}{r^4} + \frac{\hat{Y}^3g_2}{r^4} \end{bmatrix} \begin{bmatrix} u \\ v \end{bmatrix} \right) = 0$$

Since the constant vector $\mathbf{g} = (g_1, g_2)$ is arbitrary, we obtain

$$\nabla \cdot \left(\begin{bmatrix} \sigma_{11}G_{11} + \sigma_{12}G_{21} \\ \sigma_{21}G_{11} + \sigma_{22}G_{21} \end{bmatrix} + 4\mu \begin{bmatrix} \frac{\hat{X}^3u + \hat{X}^2\hat{Y}v}{r^4} \\ \frac{\hat{X}^2\hat{Y}u + \hat{X}\hat{Y}^2v}{r^4} \end{bmatrix} \right) = 0, \quad (2.15)$$

and

$$\nabla \cdot \left(\begin{bmatrix} \sigma_{11}G_{12} + \sigma_{12}G_{22} \\ \sigma_{21}G_{12} + \sigma_{22}G_{22} \end{bmatrix} + 4\mu \begin{bmatrix} \frac{\hat{X}^2\hat{Y}u + \hat{X}\hat{Y}^2v}{r^4} \\ \frac{\hat{X}\hat{Y}^2u + \hat{Y}^3v}{r^4} \end{bmatrix} \right) = 0, \quad (2.16)$$

where \mathbf{G} is the free space Green's function. In order to derive the boundary integral equation, we choose a area Ω that is bounded by a closed curve Γ , and choose a point \mathbf{X}_0 that is outside Ω . Integrating (2.15) and (2.16) over Ω , and using the divergence theorem to convert the area integral over Ω into a line integral over Γ , we obtain

$$\int_{\Gamma} \left(\begin{bmatrix} \sigma_{11}G_{11} + \sigma_{12}G_{21} \\ \sigma_{21}G_{11} + \sigma_{22}G_{21} \end{bmatrix} + 4\mu \begin{bmatrix} \frac{\hat{X}^3u + \hat{X}^2\hat{Y}v}{r^4} \\ \frac{\hat{X}^2\hat{Y}u + \hat{X}\hat{Y}^2v}{r^4} \end{bmatrix} \right) \cdot \mathbf{n} ds = 0, \quad (2.17)$$

and

$$\int_{\Gamma} \left(\begin{bmatrix} \sigma_{11}G_{12} + \sigma_{12}G_{22} \\ \sigma_{21}G_{12} + \sigma_{22}G_{22} \end{bmatrix} + 4\mu \begin{bmatrix} \frac{\hat{X}^2\hat{Y}u + \hat{X}\hat{Y}^2v}{r^4} \\ \frac{\hat{X}\hat{Y}^2u + \hat{Y}^3v}{r^4} \end{bmatrix} \right) \cdot \mathbf{n} ds = 0, \quad (2.18)$$

where $\mathbf{n} = (n_1, n_2)$ is the unit outward normal vector of Ω and s is the arclength parameter. Next, we choose a point \mathbf{X}_0 that is inside Ω . In addition, we define a small circular area $B_{\epsilon}(\mathbf{X}_0)$ that is centered at \mathbf{X}_0 with the radius ϵ . In this case, equations (2.15) and (2.16)

is regular in $\Omega \setminus B_\epsilon(\mathbf{X}_0)$. Integrating (2.15) and (2.16) over $\Omega \setminus B_\epsilon(\mathbf{X}_0)$ and using the divergence theorem again, we obtain

$$\begin{aligned} & \int_\Gamma \left(\begin{bmatrix} \sigma_{11}G_{11} + \sigma_{12}G_{21} \\ \sigma_{21}G_{11} + \sigma_{22}G_{21} \end{bmatrix} + 4\mu \begin{bmatrix} \frac{\hat{X}^3u + \hat{X}^2\hat{Y}v}{r^4} \\ \frac{\hat{X}^2\hat{Y}u + \hat{X}\hat{Y}^2v}{r^4} \end{bmatrix} \right) \cdot \mathbf{n} ds \\ &= - \int_{\partial B_\epsilon(\mathbf{X}_0)} \left(\begin{bmatrix} \sigma_{11}G_{11} + \sigma_{12}G_{21} \\ \sigma_{21}G_{11} + \sigma_{22}G_{21} \end{bmatrix} + 4\mu \begin{bmatrix} \frac{\hat{X}^3u + \hat{X}^2\hat{Y}v}{r^4} \\ \frac{\hat{X}^2\hat{Y}u + \hat{X}\hat{Y}^2v}{r^4} \end{bmatrix} \right) \cdot \mathbf{n} ds, \end{aligned}$$

and

$$\begin{aligned} & \int_\Gamma \left(\begin{bmatrix} \sigma_{11}G_{12} + \sigma_{12}G_{22} \\ \sigma_{21}G_{12} + \sigma_{22}G_{22} \end{bmatrix} + 4\mu \begin{bmatrix} \frac{\hat{X}^2\hat{Y}u + \hat{X}\hat{Y}^2v}{r^4} \\ \frac{\hat{X}\hat{Y}^2u + \hat{Y}^3v}{r^4} \end{bmatrix} \right) \cdot \mathbf{n} ds \\ &= - \int_{\partial B_\epsilon(\mathbf{X}_0)} \left(\begin{bmatrix} \sigma_{11}G_{12} + \sigma_{12}G_{22} \\ \sigma_{21}G_{12} + \sigma_{22}G_{22} \end{bmatrix} + 4\mu \begin{bmatrix} \frac{\hat{X}^2\hat{Y}u + \hat{X}\hat{Y}^2v}{r^4} \\ \frac{\hat{X}\hat{Y}^2u + \hat{Y}^3v}{r^4} \end{bmatrix} \right) \cdot \mathbf{n} ds, \end{aligned}$$

where $\partial B_\epsilon(\mathbf{X}_0)$ is the boundary of $B_\epsilon(\mathbf{X}_0)$. Letting the radius ϵ tend to zero, the right hand side of the above two integral equations tend to $-4\pi\mu u(\mathbf{X}_0)$ and $-4\pi\mu v(\mathbf{X}_0)$, respectively. Thus, we can obtain

$$\begin{aligned} \mathbf{u}(\mathbf{X}_0) &= \begin{bmatrix} u(\mathbf{X}_0) \\ v(\mathbf{X}_0) \end{bmatrix} = \frac{-1}{4\pi\mu} \int_\Gamma \begin{bmatrix} G_{11}f_1 + G_{21}f_2 \\ G_{12}f_1 + G_{22}f_2 \end{bmatrix} d\mathbf{s} \\ &+ \frac{-1}{\pi} \int_\Gamma \begin{bmatrix} u \left(\frac{\hat{X}^3n_1 + \hat{X}^2\hat{Y}n_2}{r^4} \right) + v \left(\frac{\hat{X}^2\hat{Y}n_1 + \hat{X}\hat{Y}^2n_2}{r^4} \right) \\ u \left(\frac{\hat{X}^2\hat{Y}n_1 + \hat{X}\hat{Y}^2n_2}{r^4} \right) + v \left(\frac{\hat{X}\hat{Y}^2n_1 + \hat{Y}^3n_2}{r^4} \right) \end{bmatrix} d\mathbf{s}, \end{aligned} \quad (2.19)$$

where $\hat{\mathbf{X}} = (\hat{X}, \hat{Y}) = (X - X_0, Y - Y_0)$ and $\mathbf{f} = (f_1, f_2) = \boldsymbol{\sigma}\mathbf{n}$ is the surface force. Equation (2.19) represents a flow in terms of two boundary integral involving the Green's function \mathbf{G} and the stress tensor. The first integral on the right hand side of (2.19) is called single-layer potential, and the second integral is called double-layer potential. Finally, if the source point \mathbf{X}_0 is right on the boundary Γ , we can express the velocity \mathbf{u} as

$$\begin{aligned} \mathbf{u}(\mathbf{X}_0) &= \begin{bmatrix} u(\mathbf{X}_0) \\ v(\mathbf{X}_0) \end{bmatrix} = \frac{-1}{2\pi\mu} \int_\Gamma \begin{bmatrix} G_{11}f_1 + G_{21}f_2 \\ G_{12}f_1 + G_{22}f_2 \end{bmatrix} d\mathbf{s} \\ &+ \frac{-2}{\pi} \int_\Gamma \begin{bmatrix} u \left(\frac{\hat{X}^3n_1 + \hat{X}^2\hat{Y}n_2}{r^4} \right) + v \left(\frac{\hat{X}^2\hat{Y}n_1 + \hat{X}\hat{Y}^2n_2}{r^4} \right) \\ u \left(\frac{\hat{X}^2\hat{Y}n_1 + \hat{X}\hat{Y}^2n_2}{r^4} \right) + v \left(\frac{\hat{X}\hat{Y}^2n_1 + \hat{Y}^3n_2}{r^4} \right) \end{bmatrix} d\mathbf{s}. \end{aligned} \quad (2.20)$$

In summary, equation (2.17), (2.18), (2.19) and (2.20) represent the boundary integral equations that the point \mathbf{X}_0 is outside, inside, or right on the boundary of a selected area.

In order to accelerate the numerical computation, we want to simplify the boundary integral equation by eliminating the double-layer potential. Assuming that the domain of \mathbf{u} is inside the closed curve Γ , there is a complementary flow \mathbf{u}' outside Γ . The existence

of the complementary flow \mathbf{u}' can be proved as long as the flow \mathbf{u} satisfies the following constrain

$$\int_{\Gamma} \mathbf{u} \cdot \mathbf{n} ds = 0,$$

where \mathbf{n} is the unit outward normal vector of the domain of \mathbf{u} . Furthermore, let \mathbf{u}' vanish at infinity and has the same boundary values as \mathbf{u} on Γ . On the other hand, if the domain of \mathbf{u} is outside Γ , there is a complementary flow \mathbf{u}' inside Γ so that \mathbf{u}' has the same boundary values as \mathbf{u} on Γ . In either case, we choose a point \mathbf{X}_0 inside the domain of \mathbf{u} , and use (2.17), (2.18) to find

$$\int_{\Gamma} \left(\begin{bmatrix} \sigma'_{11} G_{11} + \sigma'_{12} G_{21} \\ \sigma'_{21} G_{11} + \sigma'_{22} G_{21} \end{bmatrix} + 4\mu \begin{bmatrix} \frac{\hat{X}^3 u' + \hat{X}^2 \hat{Y} v'}{r^4} \\ \frac{\hat{X}^2 \hat{Y} u' + \hat{X} \hat{Y}^2 v'}{r^4} \end{bmatrix} \right) \cdot \mathbf{n} ds = 0, \quad (2.21)$$

and

$$\int_{\Gamma} \left(\begin{bmatrix} \sigma'_{11} G_{12} + \sigma'_{12} G_{22} \\ \sigma'_{21} G_{12} + \sigma'_{22} G_{22} \end{bmatrix} + 4\mu \begin{bmatrix} \frac{\hat{X}^2 \hat{Y} u' + \hat{X} \hat{Y}^2 v'}{r^4} \\ \frac{\hat{X} \hat{Y}^2 u' + \hat{Y}^3 v'}{r^4} \end{bmatrix} \right) \cdot \mathbf{n} ds = 0, \quad (2.22)$$

where $\mathbf{u} = (u', v')$ and σ'_{ij} is the stress tensor corresponding to \mathbf{u}' . Combining (2.21), (2.22) with (2.19), we can obtain

$$\mathbf{u}(\mathbf{X}_0) = \begin{bmatrix} u(\mathbf{X}_0) \\ v(\mathbf{X}_0) \end{bmatrix} = \frac{-1}{4\pi\bar{\mu}} \int_{\Gamma} \begin{bmatrix} G_{11} q_1 + G_{21} q_2 \\ G_{12} q_1 + G_{22} q_2 \end{bmatrix} ds, \quad (2.23)$$

where $(q_1, q_2) = \mathbf{q} = \mathbf{f} - \mathbf{f}'$. So far, we can express the flow only in terms of a single-layer potential.

2.3 Interfacial flow

Flows involving interfaces between two different fluids occur in many applications. In order to describe a interfacial flow, we consider the flow on each side of the interface. For simplicity, we label the ambient fluid and the particle fluid with Ω_1 and Ω_2 , respectively. In addition, let $\lambda = \frac{\mu_2}{\mu_1}$ be the viscosity ratio between the internal and external fluid. Using the standard boundary integral equation, which we get in the previous subsection, for a point \mathbf{X}_0 that is located outside Ω_2 , i.e., $\mathbf{X}_0 \in \Omega_1$, we can obtain

$$\begin{aligned} \mathbf{u}^1(\mathbf{X}_0) &= \begin{bmatrix} u^1(\mathbf{X}_0) \\ v^1(\mathbf{X}_0) \end{bmatrix} = \frac{-1}{4\pi\mu_1} \int_{\Gamma} \begin{bmatrix} G_{11} f_1^1 + G_{21} f_2^1 \\ G_{12} f_1^1 + G_{22} f_2^1 \end{bmatrix} ds \\ &+ \frac{-1}{\pi} \int_{\Gamma} \begin{bmatrix} u \left(\frac{\hat{X}^3 n_1 + \hat{X}^2 \hat{Y} n_2}{r^4} \right) + v \left(\frac{\hat{X}^2 \hat{Y} n_1 + \hat{X} \hat{Y}^2 n_2}{r^4} \right) \\ u \left(\frac{\hat{X}^2 \hat{Y} n_1 + \hat{X} \hat{Y}^2 n_2}{r^4} \right) + v \left(\frac{\hat{X} \hat{Y}^2 n_1 + \hat{Y}^3 n_2}{r^4} \right) \end{bmatrix} ds, \end{aligned} \quad (2.24)$$

where $\mathbf{f}^1 = (f_1^1, f_2^1)$ is the surface force over the external of Γ . On the other hand, by using equation (2.17) and (2.18) we can obtain

$$\int_{\Gamma} \begin{bmatrix} G_{11}f_1^2 + G_{21}f_2^2 \\ G_{12}f_1^2 + G_{22}f_2^2 \end{bmatrix} \mathbf{d}s + 4\mu_2 \int_{\Gamma} \begin{bmatrix} u \left(\frac{\hat{X}^3 n_1 + \hat{X}^2 \hat{Y} n_2}{r^4} \right) + v \left(\frac{\hat{X}^2 \hat{Y} n_1 + \hat{X} \hat{Y}^2 n_2}{r^4} \right) \\ u \left(\frac{\hat{X}^2 \hat{Y} n_1 + \hat{X} \hat{Y}^2 n_2}{r^4} \right) + v \left(\frac{\hat{X} \hat{Y}^2 n_1 + \hat{Y}^3 n_2}{r^4} \right) \end{bmatrix} \mathbf{d}s = 0, \quad (2.25)$$

where $\mathbf{f}^2 = (f_1^2, f_2^2)$ is the surface force over the internal of Γ . Combining (2.24) and (2.25), we find

$$\mathbf{u}^1(\mathbf{X}_0) = \begin{bmatrix} u^1(\mathbf{X}_0) \\ v^1(\mathbf{X}_0) \end{bmatrix} = \frac{-1}{4\pi\mu_1} \int_{\Gamma} \begin{bmatrix} G_{11}\Delta f_1 + G_{21}\Delta f_2 \\ G_{12}\Delta f_1 + G_{22}\Delta f_2 \end{bmatrix} \mathbf{d}s + \frac{-(1-\lambda)}{\pi} \int_{\Gamma} \begin{bmatrix} u \left(\frac{\hat{X}^3 n_1 + \hat{X}^2 \hat{Y} n_2}{r^4} \right) + v \left(\frac{\hat{X}^2 \hat{Y} n_1 + \hat{X} \hat{Y}^2 n_2}{r^4} \right) \\ u \left(\frac{\hat{X}^2 \hat{Y} n_1 + \hat{X} \hat{Y}^2 n_2}{r^4} \right) + v \left(\frac{\hat{X} \hat{Y}^2 n_1 + \hat{Y}^3 n_2}{r^4} \right) \end{bmatrix} \mathbf{d}s, \quad (2.26)$$

where $\Delta \mathbf{f} = (\Delta f_1, \Delta f_2) = \mathbf{f}^1 - \mathbf{f}^2$ is the discontinuity of the interfacial force. So far, we obtain the boundary integral equation for the external flow of the interface. Next, for a point \mathbf{X}_0 is located inside Ω_2 , using equation (2.17) and (2.18), we can obtain

$$\int_{\Gamma} \begin{bmatrix} G_{11}f_1^1 + G_{21}f_2^1 \\ G_{12}f_1^1 + G_{22}f_2^1 \end{bmatrix} \mathbf{d}s + 4\mu_1 \int_{\Gamma} \begin{bmatrix} u \left(\frac{\hat{X}^3 n_1 + \hat{X}^2 \hat{Y} n_2}{r^4} \right) + v \left(\frac{\hat{X}^2 \hat{Y} n_1 + \hat{X} \hat{Y}^2 n_2}{r^4} \right) \\ u \left(\frac{\hat{X}^2 \hat{Y} n_1 + \hat{X} \hat{Y}^2 n_2}{r^4} \right) + v \left(\frac{\hat{X} \hat{Y}^2 n_1 + \hat{Y}^3 n_2}{r^4} \right) \end{bmatrix} \mathbf{d}s = 0. \quad (2.27)$$

On the other hand, we use (2.19) to obtain

$$\mathbf{u}^2(\mathbf{X}_0) = \begin{bmatrix} u^2(\mathbf{X}_0) \\ v^2(\mathbf{X}_0) \end{bmatrix} = \frac{-1}{4\pi\mu_2} \int_{\Gamma} \begin{bmatrix} G_{11}f_1^2 + G_{21}f_2^2 \\ G_{12}f_1^2 + G_{22}f_2^2 \end{bmatrix} \mathbf{d}s + \frac{-1}{\pi} \int_{\Gamma} \begin{bmatrix} u \left(\frac{\hat{X}^3 n_1 + \hat{X}^2 \hat{Y} n_2}{r^4} \right) + v \left(\frac{\hat{X}^2 \hat{Y} n_1 + \hat{X} \hat{Y}^2 n_2}{r^4} \right) \\ u \left(\frac{\hat{X}^2 \hat{Y} n_1 + \hat{X} \hat{Y}^2 n_2}{r^4} \right) + v \left(\frac{\hat{X} \hat{Y}^2 n_1 + \hat{Y}^3 n_2}{r^4} \right) \end{bmatrix} \mathbf{d}s. \quad (2.28)$$

Combining (2.27) and (2.28), we find

$$\mathbf{u}^2(\mathbf{X}_0) = \begin{bmatrix} u^2(\mathbf{X}_0) \\ v^2(\mathbf{X}_0) \end{bmatrix} = \frac{-1}{4\pi\mu_2} \int_{\Gamma} \begin{bmatrix} G_{11}\Delta f_1 + G_{21}\Delta f_2 \\ G_{12}\Delta f_1 + G_{22}\Delta f_2 \end{bmatrix} \mathbf{d}s + \frac{-(1-\lambda)}{\pi\lambda} \int_{\Gamma} \begin{bmatrix} u \left(\frac{\hat{X}^3 n_1 + \hat{X}^2 \hat{Y} n_2}{r^4} \right) + v \left(\frac{\hat{X}^2 \hat{Y} n_1 + \hat{X} \hat{Y}^2 n_2}{r^4} \right) \\ u \left(\frac{\hat{X}^2 \hat{Y} n_1 + \hat{X} \hat{Y}^2 n_2}{r^4} \right) + v \left(\frac{\hat{X} \hat{Y}^2 n_1 + \hat{Y}^3 n_2}{r^4} \right) \end{bmatrix} \mathbf{d}s. \quad (2.29)$$

For a point \mathbf{X}_0 is located right on the interface Γ , we can obtain

$$\mathbf{u}(\mathbf{X}_0) = \begin{bmatrix} u(\mathbf{X}_0) \\ v(\mathbf{X}_0) \end{bmatrix} = \frac{-1}{2\pi\mu_1(1+\lambda)} \int_{\Gamma} \begin{bmatrix} G_{11}\Delta f_1 + G_{21}\Delta f_2 \\ G_{12}\Delta f_1 + G_{22}\Delta f_2 \end{bmatrix} \mathbf{d}s + \frac{-2(1-\lambda)}{\pi(1+\lambda)} \int_{\Gamma} \begin{bmatrix} u \left(\frac{\hat{X}^3 n_1 + \hat{X}^2 \hat{Y} n_2}{r^4} \right) + v \left(\frac{\hat{X}^2 \hat{Y} n_1 + \hat{X} \hat{Y}^2 n_2}{r^4} \right) \\ u \left(\frac{\hat{X}^2 \hat{Y} n_1 + \hat{X} \hat{Y}^2 n_2}{r^4} \right) + v \left(\frac{\hat{X} \hat{Y}^2 n_1 + \hat{Y}^3 n_2}{r^4} \right) \end{bmatrix} \mathbf{d}s. \quad (2.30)$$

It will be noted that when the viscosities of the two fluids are equal, the coefficient of the double-layer potential vanishes, and flow can be represented in terms of a single-layer potential with $\Delta \mathbf{f}$.

Next, if there is an ambient flow with velocity $\mathbf{u}^\infty = (u^\infty, v^\infty)$ past the particle fluid. The interfacial velocity $\mathbf{u}(\mathbf{X}_0)$, $\mathbf{X}_0 \in \Gamma$, can be expressed as

$$\begin{aligned} \begin{bmatrix} u(\mathbf{X}_0) \\ v(\mathbf{X}_0) \end{bmatrix} &= \frac{2}{1+\lambda} \begin{bmatrix} u^\infty \\ v^\infty \end{bmatrix} + \frac{-1}{2\pi\mu_1(1+\lambda)} \int_\Gamma \begin{bmatrix} G_{11}\Delta f_1 + G_{21}\Delta f_2 \\ G_{12}\Delta f_1 + G_{22}\Delta f_2 \end{bmatrix} ds \\ &+ \frac{-2(1-\lambda)}{\pi(1+\lambda)} \int_\Gamma \begin{bmatrix} u \left(\frac{\hat{X}^3 n_1 + \hat{X}^2 \hat{Y} n_2}{r^4} \right) + v \left(\frac{\hat{X}^2 \hat{Y} n_1 + \hat{X} \hat{Y}^2 n_2}{r^4} \right) \\ u \left(\frac{\hat{X}^2 \hat{Y} n_1 + \hat{X} \hat{Y}^2 n_2}{r^4} \right) + v \left(\frac{\hat{X} \hat{Y}^2 n_1 + \hat{Y}^3 n_2}{r^4} \right) \end{bmatrix} ds. \end{aligned} \quad (2.31)$$

So far, we obtain the boundary integral equation for interfacial velocities in two dimensional Stokes flow.

3 Numerical method

Our problem is an ambient flow with velocity \mathbf{u}^∞ past a deformable particle, where Ω_1 and Ω_2 represent the ambient fluid and the particle fluid, as illustrated in Fig. 3.1 The

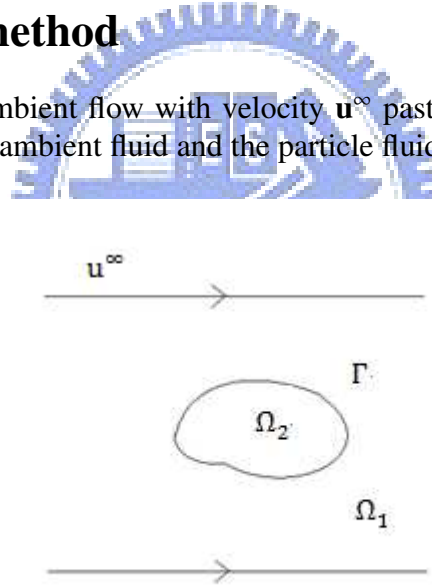


Figure 3.1: Sketch of an ambient flow past a deformable particle.

governing equations are the two dimensional steady Stokes equation with the condition of incompressibility, as following

$$-\nabla P^i + \mu_i \Delta \mathbf{u}^i = 0, \quad (3.1)$$

$$\nabla \cdot \mathbf{u}^i = 0, \quad (3.2)$$

where $i = 1, 2$. μ_1 and μ_2 are the viscosity coefficients for the ambient fluid and the particle fluid, respectively. The boundary conditions on the interface Γ between two fluids are given as following

$$\mathbf{u}^1(\mathbf{X}) = \mathbf{u}^2(\mathbf{X}), \quad (3.3)$$

$$[\boldsymbol{\sigma} \cdot \mathbf{n}](\mathbf{X}) = \mathbf{f}(\mathbf{X}), \quad (3.4)$$

where $\mathbf{X} \in \Gamma$. $\boldsymbol{\sigma}$, \mathbf{n} and \mathbf{f} are the stress tensor, the unit outward normal vector and the surface force, respectively. $[\cdot]$ denotes the discontinuity across the interface Γ . The surface force \mathbf{f} can be chosen as

$$\mathbf{f} = \frac{\partial}{\partial s}(\sigma\boldsymbol{\tau}), \quad (3.5)$$

where s is the arclength parameter, $\boldsymbol{\tau}$ is the unit tangent vector, and σ is the surface tension. Let us recall that the velocity \mathbf{u} at a point \mathbf{X}_0 on the interface Γ can be written as

$$\begin{aligned} \begin{bmatrix} u(\mathbf{X}_0) \\ v(\mathbf{X}_0) \end{bmatrix} &= \frac{2}{1+\lambda} \begin{bmatrix} u^\infty \\ v^\infty \end{bmatrix} + \frac{-1}{2\pi\mu_1(1+\lambda)} \int_\Gamma \begin{bmatrix} G_{11}f_1 + G_{21}f_2 \\ G_{12}f_1 + G_{22}f_2 \end{bmatrix} \mathbf{d}s \\ &+ \frac{-2(1-\lambda)}{\pi(1+\lambda)} \int_\Gamma \begin{bmatrix} u \left(\frac{\hat{X}^3 n_1 + \hat{X}^2 \hat{Y} n_2}{r^4} \right) + v \left(\frac{\hat{X}^2 \hat{Y} n_1 + \hat{X} \hat{Y}^2 n_2}{r^4} \right) \\ u \left(\frac{\hat{X}^2 \hat{Y} n_1 + \hat{X} \hat{Y}^2 n_2}{r^4} \right) + v \left(\frac{\hat{X} \hat{Y}^2 n_1 + \hat{Y}^3 n_2}{r^4} \right) \end{bmatrix} \mathbf{d}s, \end{aligned} \quad (3.6)$$

where $\lambda = \frac{\mu_2}{\mu_1}$ is the viscosity ratio between the particle fluid and the ambient fluid, \mathbf{G} is the two dimensional free space Green's function, and $\hat{\mathbf{X}} = (\hat{X}, \hat{Y}) = \mathbf{X} - \mathbf{X}_0$. It is obvious to see that the integral equations occur singularities when \mathbf{X} and \mathbf{X}_0 coincide. The numerical integration schemes for the integrals involving singularities will be discussed in the following subsection. Once the velocity \mathbf{u} on the interface Γ is obtained, the interfacial dynamics can be determined by

$$\frac{\partial \mathbf{X}}{\partial t} = \mathbf{u}, \quad (3.7)$$

where the interface position \mathbf{X} can be expressed as a periodic vector function of the parameter α . In summary, there are two steps for solving this interfacial dynamics problem. The first step is computing the interfacial velocity at each marker points on the interface. Then we can advance the interface by using the evolution equation (3.7) to track the positions of these marker points.

3.1 Explicit numerical integration schemes

In this subsection, we analyze the integral equation (3.6) in detail by decomposing the integrals into different terms. It is based on Xu Sun and Xiaofan Li's paper [11]. First, let

the interface Γ be parameterized by $\mathbf{X}(\alpha, t)$, where $0 \leq \alpha \leq 2\pi$. In addition, we suppress the time dependency by writing, for example, $\mathbf{X}(\alpha, t)$ as $\mathbf{X}(\alpha)$, and denote

$$\begin{aligned}\mathbf{u}(\alpha) &= \mathbf{u}(\mathbf{X}(\alpha)), \mathbf{u}(\alpha_0) = \mathbf{u}(\mathbf{X}(\alpha_0)), \\ \mathbf{G}(\alpha, \alpha_0) &= \mathbf{G}(\mathbf{X}(\alpha), \mathbf{X}(\alpha_0)).\end{aligned}$$

Then equation (3.6) can be rewritten as

$$\begin{aligned}\begin{bmatrix} u(\alpha_0) \\ v(\alpha_0) \end{bmatrix} &= \frac{2}{1+\lambda} \begin{bmatrix} u^\infty(\alpha_0) \\ v^\infty(\alpha_0) \end{bmatrix} + \frac{-1}{2\pi\mu_1(1+\lambda)} \int_\Gamma \begin{bmatrix} G_{11}(\alpha, \alpha_0)f_1(\alpha) + G_{21}(\alpha, \alpha_0)f_2(\alpha) \\ G_{12}(\alpha, \alpha_0)f_1(\alpha) + G_{22}(\alpha, \alpha_0)f_2(\alpha) \end{bmatrix} d\alpha \\ &+ \frac{-2(1-\lambda)}{\pi(1+\lambda)} \int_\Gamma \begin{bmatrix} u(\alpha) \left(\frac{\hat{X}^3 n_1(\alpha) + \hat{X}^2 \hat{Y} n_2(\alpha)}{r^4} \right) + v(\alpha) \left(\frac{\hat{X}^2 \hat{Y} n_1(\alpha) + \hat{X} \hat{Y}^2 n_2(\alpha)}{r^4} \right) \\ u(\alpha) \left(\frac{\hat{X}^2 \hat{Y} n_1(\alpha) + \hat{X} \hat{Y}^2 n_2(\alpha)}{r^4} \right) + v(\alpha) \left(\frac{\hat{X} \hat{Y}^2 n_1(\alpha) + \hat{Y}^3 n_2(\alpha)}{r^4} \right) \end{bmatrix} s_\alpha(\alpha) d\alpha,\end{aligned}\quad (3.8)$$

where $f_i(\alpha) = \frac{\partial}{\partial \alpha}(\sigma\tau_i)$, $i = 1, 2$, and $s_\alpha(\alpha) = \sqrt{X_\alpha^2 + Y_\alpha^2}$ is the stretch vector. Substituting the expression of the free space Green's function into (3.8), and rewriting

$$\ln r = \ln \left(\frac{r}{2 \sin \frac{|\alpha - \alpha_0|}{2}} \right) + \frac{1}{2} \ln \left(4 \sin^2 \frac{|\alpha - \alpha_0|}{2} \right), \quad (3.9)$$

equation (3.8) becomes

$$\begin{aligned}u(\alpha_0) &= \frac{2}{1+\lambda} u^\infty(\alpha_0) - \frac{1}{2\pi\mu_1(1+\lambda)} \int_0^{2\pi} [-f_1(\alpha)D(\alpha, \alpha_0) - \frac{1}{2}f_1(\alpha)E(\alpha, \alpha_0) \\ &+ f_1(\alpha)F_{11}(\alpha, \alpha_0) + f_2(\alpha)F_{12}(\alpha, \alpha_0)] d\alpha \\ &- \frac{2(1-\lambda)}{\pi(1+\lambda)} \int_0^{2\pi} [u(\alpha)H_{11}(\alpha, \alpha_0) + v(\alpha)H_{12}(\alpha, \alpha_0)] d\alpha\end{aligned}\quad (3.10)$$

and

$$\begin{aligned}v(\alpha_0) &= \frac{2}{1+\lambda} v^\infty(\alpha_0) - \frac{1}{2\pi\mu_1(1+\lambda)} \int_0^{2\pi} [-f_2(\alpha)D(\alpha, \alpha_0) - \frac{1}{2}f_2(\alpha)E(\alpha, \alpha_0) \\ &+ f_2(\alpha)F_{22}(\alpha, \alpha_0) + f_1(\alpha)F_{21}(\alpha, \alpha_0)] d\alpha \\ &- \frac{2(1-\lambda)}{\pi(1+\lambda)} \int_0^{2\pi} [u(\alpha)H_{21}(\alpha, \alpha_0) + v(\alpha)H_{22}(\alpha, \alpha_0)] d\alpha\end{aligned}\quad (3.11)$$

where

$$D(\alpha, \alpha_0) = \ln \left(\frac{r}{2 \sin \frac{|\alpha - \alpha_0|}{2}} \right), \quad (3.12)$$

$$E(\alpha, \alpha_0) = \ln \left(4 \sin^2 \frac{|\alpha - \alpha_0|}{2} \right), \quad (3.13)$$

$$[F_{ij}(\alpha, \alpha_0)] = \begin{bmatrix} \frac{\hat{X}^2}{r^2} & \frac{\hat{X}\hat{Y}}{r^2} \\ \frac{\hat{X}\hat{Y}}{r^2} & \frac{\hat{Y}^2}{r^2} \end{bmatrix}, \quad (3.14)$$

$$[H_{ij}(\alpha, \alpha_0)] = \begin{bmatrix} \frac{\hat{X}^3}{r^4} n_1(\alpha) s_\alpha(\alpha) + \frac{\hat{X}^2 \hat{Y}}{r^4} n_2(\alpha) s_\alpha(\alpha) & \frac{\hat{X}^2 \hat{Y}}{r^4} n_1(\alpha) s_\alpha(\alpha) + \frac{\hat{X} \hat{Y}^2}{r^4} n_2(\alpha) s_\alpha(\alpha) \\ \frac{\hat{X}^2 \hat{Y}}{r^4} n_1(\alpha) s_\alpha(\alpha) + \frac{\hat{X} \hat{Y}^2}{r^4} n_2(\alpha) s_\alpha(\alpha) & \frac{\hat{X} \hat{Y}^2}{r^4} n_1(\alpha) s_\alpha(\alpha) + \frac{\hat{Y}^3}{r^4} n_2(\alpha) s_\alpha(\alpha) \end{bmatrix}, \quad (3.15)$$

in which $\hat{X} = X(\alpha) - X(\alpha_0)$, $\hat{Y} = Y(\alpha) - Y(\alpha_0)$ and $r = \sqrt{\hat{X}^2 + \hat{Y}^2}$.

Assuming that the interface curve Γ is of $C^\infty[0, 2\pi]$, we can find the limits of (3.12), (3.14) and (3.15) when the source point \mathbf{X}_0 and the observation point \mathbf{X} coincide, i.e., $\alpha \rightarrow \alpha_0$. By using the Taylor expansion of $\mathbf{X}(\alpha) - \mathbf{X}(\alpha_0)$ and $\sin \frac{|\alpha - \alpha_0|}{2}$, we have

$$\begin{aligned} D(\alpha_0, \alpha_0) &= \ln \left(\frac{\sqrt{\left[\sum_{n=1}^{\infty} \frac{x^{(n)}(\alpha_0)(\alpha - \alpha_0)^n}{n!} \right]^2 + \left[\sum_{n=1}^{\infty} \frac{y^{(n)}(\alpha_0)(\alpha - \alpha_0)^n}{n!} \right]^2}}{2 \sum_{n=1}^{\infty} \frac{(-1)^{n+1}}{(2n-1)!} \left(\frac{|\alpha - \alpha_0|}{2} \right)^{2n-1}} \right) \\ &= \ln \left(\frac{\sqrt{\left[\sum_{n=1}^{\infty} \frac{x^{(n)}(\alpha_0)(\alpha - \alpha_0)^{n-1}}{n!} \right]^2 + \left[\sum_{n=1}^{\infty} \frac{y^{(n)}(\alpha_0)(\alpha - \alpha_0)^{n-1}}{n!} \right]^2}}{1 + \sum_{n=1}^{\infty} \frac{(-1)^{n+1}}{(2n-1)!} \left(\frac{|\alpha - \alpha_0|}{2} \right)^{2n-2}} \right) \end{aligned} \quad (3.16)$$

It will be noted that the denominator of (3.16) does not vanish when $\alpha = \alpha_0$. Discarding the high order term, we can obtain

$$D(\alpha_0, \alpha_0) = \lim_{\alpha \rightarrow \alpha_0} D(\alpha, \alpha_0) = \ln(s_\alpha(\alpha_0)). \quad (3.17)$$

Similarly,

$$[F_{ij}(\alpha_0, \alpha_0)] = \lim_{\alpha \rightarrow \alpha_0} [F_{ij}(\alpha, \alpha_0)] = \begin{bmatrix} \tau_1(\alpha_0)^2 & \tau_1(\alpha_0)\tau_2(\alpha_0) \\ \tau_1(\alpha_0)\tau_2(\alpha_0) & \tau_2(\alpha_0)^2 \end{bmatrix}, \quad (3.18)$$

$$[H_{ij}(\alpha_0, \alpha_0)] = \lim_{\alpha \rightarrow \alpha_0} [H_{ij}(\alpha, \alpha_0)] = \begin{bmatrix} \frac{\kappa(\alpha_0)X_\alpha^2(\alpha_0)}{2s_\alpha(\alpha_0)} & \frac{\kappa(\alpha_0)X_\alpha(\alpha_0)Y_\alpha(\alpha_0)}{2s_\alpha(\alpha_0)} \\ \frac{\kappa(\alpha_0)X_\alpha(\alpha_0)Y_\alpha(\alpha_0)}{2s_\alpha(\alpha_0)} & \frac{\kappa(\alpha_0)Y_\alpha^2(\alpha_0)}{2s_\alpha(\alpha_0)} \end{bmatrix}, \quad (3.19)$$

where $\boldsymbol{\tau} = (\tau_1, \tau_2)$ is the unit tangent vector along the interface Γ and κ is the curvature of the interface Γ . Let us divide the interval $[0, 2\pi]$ evenly by $2N$ segments and denote $\alpha_j = j\pi/N$, where $j = 0, 1, \dots, 2N - 1$, and choose $M = 2N$. As a consequence, the integrals concerning (3.12), (3.14) and (3.15) can be computed by using the trapezoidal rule. Next, let us consider the integral

$$\int_0^{2\pi} -\frac{1}{2}f_k(\alpha)E(\alpha, \alpha_0)d\alpha, \quad k = 1, 2. \quad (3.20)$$

Choosing α_0 to be one of α_j 's, $\alpha_0 = \alpha_i$, we can approximate the weakly singular integral (3.20) with the following quadrature [5]

$$\int_0^{2\pi} -\frac{1}{2}f_k(\alpha) \ln\left(4 \sin^2 \frac{|\alpha - \alpha_0|}{2}\right) d\alpha \approx \Delta\alpha \sum_{j=0}^{M-1} \frac{-1}{2}R_{|j-i|}^{(\frac{M}{2})}f_k(\alpha_j), \quad (3.21)$$

where the quadrature weights are given by

$$R_q^{(N)} = -2 \left(\sum_{p=1}^{N-1} \frac{1}{p} \cos \frac{pq\pi}{N} + \frac{(-1)^q}{2N} \right), \quad q = 0, 1, \dots, 2N - 1. \quad (3.22)$$

Thus, the explicit numerical integration schemes are

$$\begin{aligned} U_i^{n+1} = & \frac{2}{1+\lambda}U_i^\infty - \frac{\Delta\alpha}{2\pi\mu_1(1+\lambda)} \sum_{j=0}^{M-1} [-D(\alpha_j, \alpha_i)(f_1)_j^n \\ & + \frac{-1}{2}R_{|j-i|}^{(\frac{M}{2})}(f_1)_j^n + F_{11}(\alpha_j, \alpha_i)(f_1)_j^n + F_{12}(\alpha_j, \alpha_i)(f_2)_j^n] \\ & - \frac{2\Delta\alpha(1-\lambda)}{\pi(1+\lambda)} \sum_{j=0}^{M-1} H_{11}(\alpha_j, \alpha_i)U_j^{n+1} + H_{12}(\alpha_j, \alpha_i)V_j^{n+1}, \end{aligned} \quad (3.23)$$

and

$$\begin{aligned} V_i^{n+1} = & \frac{2}{1+\lambda}V_i^\infty - \frac{\Delta\alpha}{2\pi\mu_1(1+\lambda)} \sum_{j=0}^{M-1} [-D(\alpha_j, \alpha_i)(f_2)_j^n \\ & + \frac{-1}{2}R_{|j-i|}^{(\frac{M}{2})}(f_2)_j^n + F_{22}(\alpha_j, \alpha_i)(f_2)_j^n + F_{21}(\alpha_j, \alpha_i)(f_1)_j^n] \\ & - \frac{2\Delta\alpha(1-\lambda)}{\pi(1+\lambda)} \sum_{j=0}^{M-1} H_{21}(\alpha_j, \alpha_i)U_j^{n+1} + H_{22}(\alpha_j, \alpha_i)V_j^{n+1}, \end{aligned} \quad (3.24)$$

where U_i^{n+1} and V_i^{n+1} denote the numerical approximation to $u(\alpha_0)$ and $v(\alpha_0)$ at next time step. Recalling that when the viscosities of the two fluids are equal, i.e., $\lambda = 1$, the coefficient of the double-layer potential vanishes, the numerical integration scheme can be

represented only in terms of the single-layer potential. On the other hand, if the viscosities of the two fluids are different, we obtain a dense linear system for the velocity U_i^{n+1} and V_i^{n+1} , and the size of this linear system is twice of the number of the marker points on the interface. Consequently, the subroutine in the IMSL math library for fortran 95 is employed to solve the linear system. If the velocity U^{n+1} and V^{n+1} is obtained, the interface dynamics can be determined by using the following equation to track the positions of the marker points on the interface,

$$\frac{\mathbf{X}_i^{n+1} - \mathbf{X}_i^n}{\Delta t} = \mathbf{u}_i^{n+1}.$$

3.2 Implicit numerical integration schemes

There are many literatures studying to remove the stiffness [1, 2, 3]. In order to remove the stiffness in our problem, we derive implicit schemes based on the boundary integral equation case by case. In the first case, which is Stokes flow with the elastic force, the surface force \mathbf{f} is expressed as

$$\mathbf{f} = \frac{\partial}{\partial s}(\sigma \boldsymbol{\tau}),$$

where s is the arclength parameter, $\boldsymbol{\tau}$ is the unit tangent vector, and the surface tension σ is computed by Hook's law

$$\sigma = s_b(s_\alpha - r_0),$$

in which, s_b is the elastic coefficient of the boundary and r_0 is the rest length. Then we can discretize the surface tension term by $\sigma_j^{n+1} = s_b((s_\alpha)_j^{n+1} - r_0)$. Using the center difference to discretize the elastic force terms ($f_1(\alpha)$, $f_2(\alpha)$) and substituting those expressions into (3.23) and (3.24), we obtain

$$\begin{aligned} U_i^{n+1} = & \frac{2}{1+\lambda} U_i^\infty + C_1 \sum_{j=0}^{M-1} [-D(\alpha_j, \alpha_i) + \frac{-1}{2} R_{|j-i|}^{(\frac{M}{2})} + F_{11}(\alpha_j, \alpha_i)] [\sigma_{j+1}^{n+1}(\tau_1)_{j+1}^n - \sigma_j^{n+1}(\tau_1)_j^n] \\ & + F_{12}(\alpha_j, \alpha_i) [\sigma_{j+1}^{n+1}(\tau_2)_{j+1}^n - \sigma_j^{n+1}(\tau_2)_j^n] + C_2 \sum_{j=0}^{M-1} H_{11}(\alpha_j, \alpha_i) U_j^{n+1} + H_{12}(\alpha_j, \alpha_i) V_j^{n+1}, \end{aligned} \quad (3.25)$$

and

$$\begin{aligned} V_i^{n+1} = & \frac{2}{1+\lambda} V_i^\infty + C_1 \sum_{j=0}^{M-1} [-D(\alpha_j, \alpha_i) + \frac{-1}{2} R_{|j-i|}^{(\frac{M}{2})} + F_{22}(\alpha_j, \alpha_i)] [\sigma_{j+1}^{n+1}(\tau_2)_{j+1}^n - \sigma_j^{n+1}(\tau_2)_j^n] \\ & + F_{21}(\alpha_j, \alpha_i) [\sigma_{j+1}^{n+1}(\tau_1)_{j+1}^n - \sigma_j^{n+1}(\tau_1)_j^n] + C_2 \sum_{j=0}^{M-1} H_{21}(\alpha_j, \alpha_i) U_j^{n+1} + H_{22}(\alpha_j, \alpha_i) V_j^{n+1}, \end{aligned} \quad (3.26)$$

where $C_1 = \frac{-1}{2\pi\mu_1(1+\lambda)}$ and $C_2 = \frac{-2\Delta\alpha(1-\lambda)}{\pi(1+\lambda)}$. Using the summation by part, equations (3.25) and (3.26) become

$$\begin{aligned}
U_i^{n+1} &= \frac{2}{1+\lambda} U_i^\infty + \hat{C}_1 \sum_{j=0}^{M-1} (A_{i,j-1} - A_{i,j})(\tau_1)_j^n (s_\alpha)_j^{n+1} + (B_{i,j-1} - B_{i,j})(\tau_2)_j^n (s_\alpha)_j^{n+1} \\
&+ C_2 \sum_{j=0}^{M-1} H_{11}(\alpha_j, \alpha_i) U_j^{n+1} + H_{12}(\alpha_j, \alpha_i) V_j^{n+1} \\
&- \bar{C}_1 \sum_{j=0}^{M-1} (A_{i,j-1} - A_{i,j})(\tau_1)_j^n + (B_{i,j-1} - B_{i,j})(\tau_2)_j^n,
\end{aligned} \tag{3.27}$$

and

$$\begin{aligned}
V_i^{n+1} &= \frac{2}{1+\lambda} V_i^\infty + \hat{C}_1 \sum_{j=0}^{M-1} (C_{i,j-1} - C_{i,j})(\tau_2)_j^n (s_\alpha)_j^{n+1} + (B_{i,j-1} - B_{i,j})(\tau_1)_j^n (s_\alpha)_j^{n+1} \\
&+ C_2 \sum_{j=0}^{M-1} H_{21}(\alpha_j, \alpha_i) U_j^{n+1} + H_{22}(\alpha_j, \alpha_i) V_j^{n+1} \\
&- \bar{C}_1 \sum_{j=0}^{M-1} (C_{i,j-1} - C_{i,j})(\tau_2)_j^n + (B_{i,j-1} - B_{i,j})(\tau_1)_j^n,
\end{aligned} \tag{3.28}$$

where $\hat{C}_1 = C_1 s_b$, $\bar{C}_1 = C_1 s_b r_0$, $A_{i,j} = -D(\alpha_j, \alpha_i) + \frac{-1}{2} R_{|j-i|}^{(\frac{M}{2})} + F_{11}(\alpha_j, \alpha_i)$, $B_{i,j} = F_{12}(\alpha_j, \alpha_i) = F_{21}(\alpha_j, \alpha_i)$, and $C_{i,j} = -D(\alpha_j, \alpha_i) + \frac{-1}{2} R_{|j-i|}^{(\frac{M}{2})} + F_{22}(\alpha_j, \alpha_i)$. In addition, we use the identity

$$\frac{\partial}{\partial t} s_\alpha = \frac{X_\alpha X_{\alpha t} + Y_\alpha Y_{\alpha t}}{s_\alpha} = \frac{X_\alpha u_\alpha + Y_\alpha v_\alpha}{s_\alpha} = \frac{\partial \mathbf{u}}{\partial \alpha} \cdot \boldsymbol{\tau}. \tag{3.29}$$

Equation (3.29) can be discretized as following

$$\frac{(s_\alpha)_i^{n+1} - (s_\alpha)_i^n}{\Delta t} = \frac{\mathbf{u}_i^{n+1} - \mathbf{u}_{i-1}^{n+1}}{\Delta \alpha} \cdot \boldsymbol{\tau}_i^n. \tag{3.30}$$

Coupling the boundary equation (3.27) and (3.28) with (3.30), there is a linear system for the velocity U_i^{n+1} , V_i^{n+1} and the stretch vector $(s_\alpha)_i^{n+1}$, as following

$$\begin{bmatrix} \hat{H}_{11} + I_M & \hat{H}_{12} & D_1 \\ \hat{H}_{21} & \hat{H}_{22} + I_M & D_2 \\ L_1 & L_2 & I_M \end{bmatrix} \begin{bmatrix} U^{n+1} \\ V^{n+1} \\ (s_\alpha)^{n+1} \end{bmatrix} = \begin{bmatrix} rhs_1 \\ rhs_2 \\ rhs_3 \end{bmatrix}, \tag{3.31}$$

where

$$\begin{aligned}
(\hat{H}_{11})_{ij} &= C_2 H_{11}(\alpha_j, \alpha_i), & (\hat{H}_{12})_{ij} &= C_2 H_{12}(\alpha_j, \alpha_i), \\
(\hat{H}_{21})_{ij} &= C_2 H_{21}(\alpha_j, \alpha_i), & (\hat{H}_{22})_{ij} &= C_2 H_{22}(\alpha_j, \alpha_i), \\
(D_1)_{ij} &= \hat{C}_1 (A_{i,j-1} - A_{i,j})(\tau_1)_j^n + \hat{C}_1 (B_{i,j-1} - B_{i,j})(\tau_1)_j^n, \\
(D_2)_{ij} &= \hat{C}_1 (C_{i,j-1} - C_{i,j})(\tau_2)_j^n + \hat{C}_1 (B_{i,j-1} - B_{i,j})(\tau_2)_j^n, \\
(rhs_1)_i &= \frac{2}{1+\lambda} U_i^\infty - \bar{C}_1 \sum_{j=0}^{M-1} (A_{i,j-1} - A_{i,j})(\tau_1)_j^n + (B_{i,j-1} - B_{i,j})(\tau_2)_j^n, \\
(rhs_2)_i &= \frac{2}{1+\lambda} V_i^\infty - \bar{C}_1 \sum_{j=0}^{M-1} (C_{i,j-1} - C_{i,j})(\tau_2)_j^n + (B_{i,j-1} - B_{i,j})(\tau_1)_j^n, \\
(rhs_3)_i &= (s_\alpha)_i^n, \\
L_1 &= \begin{bmatrix} \frac{-\Delta t}{\Delta s}(\tau_1)_0 & 0 \dots 0 & \frac{\Delta t}{\Delta s}(\tau_1)_0 \\ \frac{\Delta t}{\Delta s}(\tau_1)_1 & \frac{-\Delta t}{\Delta s}(\tau_1)_1 & 0 \dots 0 \\ \vdots & \vdots & \vdots \\ 0 \dots 0 & \frac{\Delta t}{\Delta s}(\tau_1)_{M-1} & \frac{-\Delta t}{\Delta s}(\tau_1)_{M-1} \end{bmatrix}, \\
L_2 &= \begin{bmatrix} \frac{-\Delta t}{\Delta s}(\tau_2)_0 & 0 \dots 0 & \frac{\Delta t}{\Delta s}(\tau_2)_0 \\ \frac{\Delta t}{\Delta s}(\tau_2)_1 & \frac{-\Delta t}{\Delta s}(\tau_2)_1 & 0 \dots 0 \\ \vdots & \vdots & \vdots \\ 0 \dots 0 & \frac{\Delta t}{\Delta s}(\tau_2)_{M-1} & \frac{-\Delta t}{\Delta s}(\tau_2)_{M-1} \end{bmatrix},
\end{aligned}$$

and I_M is the $M \times M$ identity matrix. In addition, $\hat{H}_{11}, \hat{H}_{12}, \hat{H}_{21}, \hat{H}_{22}, D_1$, and D_2 are $M \times M$ dense matrices, and the size of this linear system is triple of the number of the marker points on the interface. The linear system (3.31) can be solve by the method that is provided from the IMSL math library for fortran 95. It will be noted that when the viscosity ratio λ is equal to 1, the numerical integration scheme can be represented only in terms of the single-layer potential. Thus, the linear system (3.31) reduce to

$$\begin{bmatrix} I_M & 0 & D_1 \\ 0 & I_M & D_2 \\ L_1 & L_2 & I_M \end{bmatrix} \begin{bmatrix} U^{n+1} \\ V^{n+1} \\ (s_\alpha)^{n+1} \end{bmatrix} = \begin{bmatrix} rhs_1 \\ rhs_2 \\ rhs_3 \end{bmatrix}. \quad (3.32)$$

In this case, the Gauss elimination method is be chosen to solve the linear system (3.32).

Step 1. observing the linear system (3.32), we can obtain

$$\begin{aligned}
U^{n+1} + D_1 (s_\alpha)^{n+1} &= rhs_1, \\
V^{n+1} + D_2 (s_\alpha)^{n+1} &= rhs_2, \\
L_1 U^{n+1} + L_2 V^{n+1} + (s_\alpha)^{n+1} &= rhs_3.
\end{aligned}$$

Step 2. solving the following linear system to obtain the stretch vector $(s_\alpha)^{n+1}$,

$$(I_M - L_1 D_1 - L_2 D_2)(s_\alpha)^{n+1} = rhs_3 - L_1 rhs_1 - L_2 rhs_2.$$

Step 3. substituting $(s_\alpha)^{n+1}$ into Step 1 to obtain the velocity U^{n+1} and V^{n+1} ,

$$\begin{aligned} U^{n+1} &= rhs_1 - D_1(s_\alpha)^{n+1}, \\ V^{n+1} &= rhs_2 - D_2(s_\alpha)^{n+1}. \end{aligned}$$

In the second case, which is an inextensible vesicle suspended in Stokes flow, we also can derive implicit numerical integration schemes. By real experiments and observations, scientists discover that the surface area of a blood cell is conserved during the process of the deformation. In two dimensional case, there is one more constrain that is the condition of inextensibility $\nabla_s \cdot \mathbf{u} = 0$. This constrain comes from the real observation and experiment. In order to let the flow satisfy the condition of inextensibility, we use the function σ to be a Lagrange multiplier for this constrain. The surface force terms (f_1, f_2) can be discretized as $(\frac{\partial(\sigma^{n+1}(\tau_1)^n)}{\partial\alpha}, \frac{\partial(\sigma^{n+1}(\tau_2)^n)}{\partial\alpha})$. Substituting these expressions into the boundary integral equation (3.23) and (3.24) and using the summation by part, we find

$$\begin{aligned} U_i^{n+1} &= \frac{2}{1+\lambda} U_i^\infty + C_1 \sum_{j=0}^{M-1} (A_{i,j-1} - A_{i,j})(\tau_1)_j^n \sigma_j^{n+1} + (B_{i,j-1} - B_{i,j})(\tau_2)_j^n \sigma_j^{n+1} \\ &+ C_2 \sum_{j=0}^{M-1} H_{11}(\alpha_j, \alpha_i) U_j^{n+1} + H_{12}(\alpha_j, \alpha_i) V_j^{n+1}, \end{aligned} \quad (3.33)$$

and

$$\begin{aligned} V_i^{n+1} &= \frac{2}{1+\lambda} V_i^\infty + C_1 \sum_{j=0}^{M-1} (C_{i,j-1} - C_{i,j})(\tau_2)_j^n \sigma_j^{n+1} + (B_{i,j-1} - B_{i,j})(\tau_1)_j^n \sigma_j^{n+1} \\ &+ C_2 \sum_{j=0}^{M-1} H_{21}(\alpha_j, \alpha_i) U_j^{n+1} + H_{22}(\alpha_j, \alpha_i) V_j^{n+1}. \end{aligned} \quad (3.34)$$

Furthermore, the condition of inextensibility $\nabla_s \cdot \mathbf{u} = 0$ can be discretized as

$$\frac{\mathbf{u}_i^{n+1} - \mathbf{u}_{i-1}^{n+1}}{\Delta\alpha} \cdot \boldsymbol{\tau}_i^n = 0. \quad (3.35)$$

Combining (3.33) and (3.34) with (3.35), we find the linear system for the vesicle flow

$$\begin{bmatrix} \hat{H}_{11} + I_M & \hat{H}_{12} & D_1 \\ \hat{H}_{21} & \hat{H}_{22} + I_M & D_2 \\ \hat{L}_1 & \hat{L}_2 & 0 \end{bmatrix} \begin{bmatrix} U^{n+1} \\ V^{n+1} \\ \sigma^{n+1} \end{bmatrix} = \begin{bmatrix} r\hat{h}s_1 \\ r\hat{h}s_2 \\ 0 \end{bmatrix}, \quad (3.36)$$

where

$$\begin{aligned} r\hat{h}s_{1i} &= \frac{2}{1+\lambda}U_i^\infty, \quad r\hat{h}s_{2i} = \frac{2}{1+\lambda}V_i^\infty, \\ \hat{L}_1 &= \begin{bmatrix} (\tau_1)_0 & 0 \dots 0 & -(\tau_1)_0 \\ -(\tau_1)_1 & (\tau_1)_1 & 0 \dots 0 \\ & \ddots & \\ 0 \dots 0 & -(\tau_1)_{M-1} & (\tau_1)_{M-1} \end{bmatrix}, \\ \hat{L}_2 &= \begin{bmatrix} (\tau_2)_0 & 0 \dots 0 & -(\tau_2)_0 \\ -(\tau_2)_1 & (\tau_2)_1 & 0 \dots 0 \\ & \ddots & \\ 0 \dots 0 & -(\tau_2)_{M-1} & (\tau_2)_{M-1} \end{bmatrix}. \end{aligned}$$

The size of (3.36) is equal to the size of (3.31). The subroutine in the IMSL math library for fortran 95 is employed to solve the linear system (3.36). When the viscosity ratio λ is equal to 1, the coefficient of the double-layer potential vanishes. The linear system (3.36) reduce to

$$\begin{bmatrix} I_M & 0 & -D_1 \\ 0 & I_M & -D_2 \\ \hat{L}_1 & \hat{L}_2 & 0 \end{bmatrix} \begin{bmatrix} U^{n+1} \\ V^{n+1} \\ \sigma^{n+1} \end{bmatrix} = \begin{bmatrix} r\hat{h}s_1 \\ r\hat{h}s_2 \\ 0 \end{bmatrix}. \quad (3.37)$$

The linear system (3.37) can be solved by the Gauss elimination method as the following steps:

Step 1. observing the linear system (3.37), we can obtain

$$\begin{aligned} U^{n+1} + D_1\sigma^{n+1} &= r\hat{h}s_1, \\ V^{n+1} + D_2\sigma^{n+1} &= r\hat{h}s_2, \\ \hat{L}_1U^{n+1} + \hat{L}_2V^{n+1} &= 0. \end{aligned}$$

Step 2. solving the following linear system to obtain the surface tension σ^{n+1} ,

$$(\hat{L}_1D_1 + \hat{L}_2D_2)\sigma^{n+1} = \hat{L}_1r\hat{h}s_1 + \hat{L}_2r\hat{h}s_2.$$

Step 3. substituting σ^{n+1} into Step 1 to obtain the velocity U^{n+1} and V^{n+1} ,

$$\begin{aligned} U^{n+1} &= r\hat{h}s_1 - D_1\sigma^{n+1}, \\ V^{n+1} &= r\hat{h}s_2 - D_2\sigma^{n+1}. \end{aligned}$$

Once the velocity U^{n+1} and V^{n+1} is obtained by solving one of the above linear systems, the interface dynamics can be determined by using the following equation to track the positions of the marker points on the interface,

$$\frac{\mathbf{X}_i^{n+1} - \mathbf{X}_i^n}{\Delta t} = \mathbf{u}_i^{n+1}.$$

4 Numerical result

We will perform a number of numerical experiments to simulate the interfacial dynamics and to test the convergence of our explicit and implicit numerical integration schemes for Stokes flow. Moreover, an example of simulating the motion of an inextensible vesicle in Stokes flow is presented in this section.

4.1 Stokes flow with elastic force

The test problem we use is one typically seen in the literature, in which the boundary is a closed curve initially in the shape of an ellipse. We choose an ellipse initially aligned in the coordinate directions with horizontal semi-axis a and vertical semi-axis b . The boundary can be parameterized as

$$\begin{cases} X(\alpha, 0) = a \cos(\alpha), \\ Y(\alpha, 0) = b \sin(\alpha). \end{cases}$$

Let the ambient flow $\mathbf{u}^\infty = 0$. For the initial condition defined as above, the steady state of the boundary is a circle with radius $r = \sqrt{ab}$ and the rest length r_0 is chosen as $\min(a, b)$. The area is conserved during the time evolution since the flow is incompressible. We present two test cases in this subsection. In the first test case, we consider the interfacial dynamics when the fluid viscosity ratio λ is equal to 1 ($\mu_1 = \mu_2 = 1$). Fig. 4.1 shows the boundary configurations obtained by the explicit scheme and implicit scheme at different time steps. The equilibrium configuration is a circle and the results of two schemes are the same. The convergence tests corresponding to the explicit scheme and the implicit scheme are shown in Table 4.1 and Table 4.2, respectively. Here we take the maximum norm for the error of the velocity (U_h, V_h) , and define the convergence order(M) by $\text{order}(M) = \log_2 \left(\frac{\text{error}(M/2)}{\text{error}(M)} \right)$. Shown from the data, as the resolution increases, the magnitude of the error decreases. For the second test case, we simulate the interfacial dynamics when $\mu_1 = 1$ and $\mu_2 = 10$, i.e., the fluid viscosity ratio $\lambda = 10$. In Fig. 4.2, we plot the boundary configurations obtained by the explicit scheme and implicit scheme at different time steps. In our numerical results, the larger the viscosity ratio λ is, the slower the interface configuration goes to equilibrium, because the coefficients of the boundary integral equations are some types of $\frac{1}{1+\lambda}$. The convergence tests corresponding to the explicit scheme and the implicit scheme are shown in Table 4.3 and Table 4.4, respectively. In the above two cases, we take $\Delta t = (\min(s_\alpha)\Delta\alpha)^2$ for the explicit schemes and take $\Delta t = \min(s_\alpha)\Delta\alpha$ for the implicit schemes. However, when the implicit schemes are used, the magnitude of the error decreases only first order. In Table 4.5, we present a stability test for our explicit scheme and our implicit scheme when s_b is equal to 10^3 , 10^4 , 10^5 and $\mu_1 = \mu_2 = 1$. In this case, the computational cost of our implicit scheme is large, i.e., Δt is small.

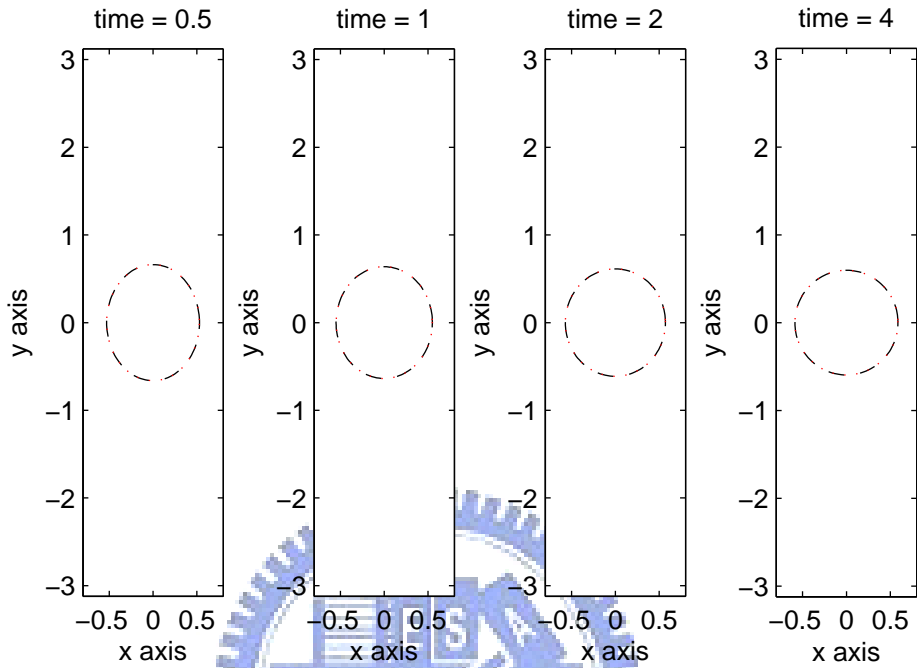


Figure 4.1: The interfacial dynamics of the time evolution for $a = 0.5, b = 0.7, s_b = 10, \mu_1 = \mu_2 = 1$, and $M = 128$. Dotted line: the explicit scheme; Dashed line: the implicit scheme.

Table 4.1: The mesh refinement results for the velocity (U_h, V_h) and the relative error of the enclosed area A_h for the explicit scheme at $T = 0.1$.

M	$\ U_{512} - U_h\ _\infty$	order	$\ V_{512} - V_h\ _\infty$	order	$ A_0 - A_h /A_0$	order
64	5.77e-4	-	6.66e-4	-	1.61e-3	-
128	1.38e-4	2.06	1.61e-4	2.05	4.04e-4	2.00
256	2.77e-5	2.32	3.23e-5	2.31	1.01e-4	2.00

Table 4.2: The mesh refinement results for the velocity (U_h, V_h) and the relative error of the enclosed area A_h for the implicit scheme at $T = 0.1$.

M	$\ U_{512} - U_h\ _\infty$	order	$\ V_{512} - V_h\ _\infty$	order	$ A_0 - A_h /A_0$	order
64	3.00e-3	-	5.15e-3	-	1.69e-3	-
128	1.41e-3	1.09	2.32e-3	1.15	4.42e-4	1.93
256	4.90e-4	1.53	7.89e-4	1.55	1.19e-4	1.89

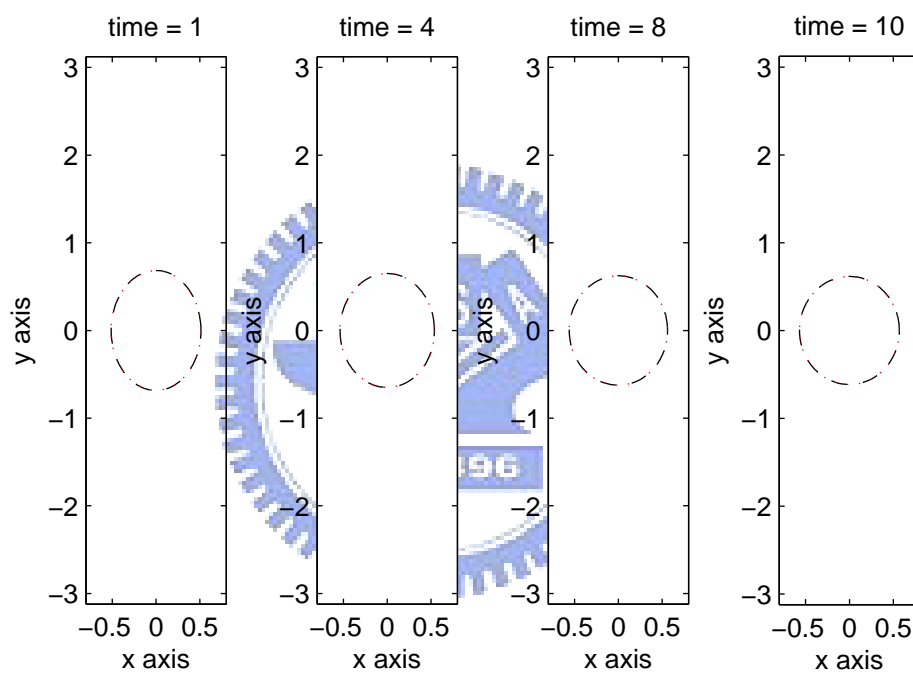


Figure 4.2: The interfacial dynamics of the time evolution for $a = 0.5, b = 0.7, s_b = 10, \mu_1 = 1, \mu_2 = 10$, and $M = 128$. Dotted line: the explicit scheme; Dashed line: the implicit scheme.

Table 4.3: The mesh refinement results for the velocity (U_h, V_h) and the relative error of the enclosed area A_h for the explicit scheme at $T = 0.1$.

M	$\ U_{512} - U_h\ _\infty$	order	$\ V_{512} - V_h\ _\infty$	order	$ A_0 - A_h /A_0$	order
64	4.58e-5	-	7.57e-5	-	1.62e-3	-
128	1.06e-5	2.11	1.80e-5	2.07	4.04e-4	2.00
256	2.10e-6	2.34	3.61e-6	2.32	1.01e-4	2.00

Table 4.4: The mesh refinement results for the velocity (U_h, V_h) and the relative error of the enclosed area A_h for the implicit scheme at $T = 0.1$.

M	$\ U_{512} - U_h\ _\infty$	order	$\ V_{512} - V_h\ _\infty$	order	$ A_0 - A_h /A_0$	order
64	1.11e-4	-	1.85e-4	-	1.61e-3	-
128	4.92e-5	1.17	7.79e-5	1.25	4.03e-4	2.00
256	1.66e-5	1.56	2.57e-5	1.60	1.01e-4	1.99

Table 4.5: The stability test for our explicit scheme and our implicit scheme when s_b is equal to $10^3, 10^4, 10^5$ and $\mu_1 = \mu_2 = 1$ for $M = 128$.

s_b	10^3	10^4	10^5
Δt_{exp}	6.02e-6	2.41e-7	6.02e-8
Δt_{imp}	3.93e-3	4.91e-4	4.91e-6

4.2 Vesicle in Shear flow

In this subsection, the initial shape in the subsection 4.1 is used to simulate the motion of a vesicle and we also presented two test cases. In the first case, we consider that a vesicle suspended in a simple shear flow with the shear rate γ is equal to 1. If the interior and the exterior of the vesicle are filled with the same fluid, the vesicle undergoes a tank-treading motion at its equilibrium configuration. Here we choose the viscosity $\mu_1 = \mu_2 = 1$ and take $\Delta t = \min(s_\alpha)\Delta\alpha$. In Fig. 4.3, we simulate a tank-treading motion of a vesicle in a simple shear flow. The convergence test for the velocity (U_h, V_h) and the surface tension σ_h is shown in Table 4.6. The reduced area V is defined as $\frac{4\pi A_0}{(L_0)^2}$, where A_0 is the initial enclosed area and L_0 is the initial arclength. The inclination angle θ/π and the tank-treading frequency $F = \frac{2\pi}{\int \frac{1}{u^2} ds}$ versus the reduced area V with different shear rate γ are shown in Fig. 4.4. As we can see, the inclination angle is independent of the shear rate, but the tank-treading frequency is dependent. In Fig. 4.5, we plot the relative error of the enclosed area A_h and the arclength L_h for time evolution. For the second test case, we also consider an inextensible vesicle suspended in a simple shear flow, but the viscosity of the interior fluid is different with the viscosity of the exterior fluid. The

initial shape of the interface is an ellipse with horizontal semi-axis $a = 0.5$ and vertical semi-axis $b = 0.7$. We choose the shear rate γ is equal to 1 and the viscosity λ is equal to 3 ($\mu_1 = 1, \mu_2 = 3$), and take $\Delta t = \min(s_\alpha)\Delta\alpha$. In Fig. 4.6, we simulate a tank-treading motion of a vesicle, and the convergence for the velocity (U_h, V_h) and the surface tension σ_h is shown in Table 4.7. In Fig. 4.7, we plot the relative error of the enclosed area A_h and the arclength L_h for time evolution. Next, we replace the viscosity ratio $\lambda = 3$ ($\mu_1 = 1, \mu_2 = 3$) with $\lambda = 10$ ($\mu_1 = 1, \mu_2 = 10$), then the vesicle undergoes a tumbling motion at its equilibrium configuration. In Fig. 4.8, we simulate a tumbling motion of a vesicle in a simple shear flow with the shear rate γ is equal to 1. The convergence test for the velocity (U_h, V_h) and the surface tension σ_h is shown in Table 4.8. In Fig. 4.9, we plot the relative error of the enclosed area A_h and the arclength L_h for time evolution. The boundary of the numerical results between the tank-treading motion (lower part) and the tumbling motion (upper part) is shown in Fig. 4.10.

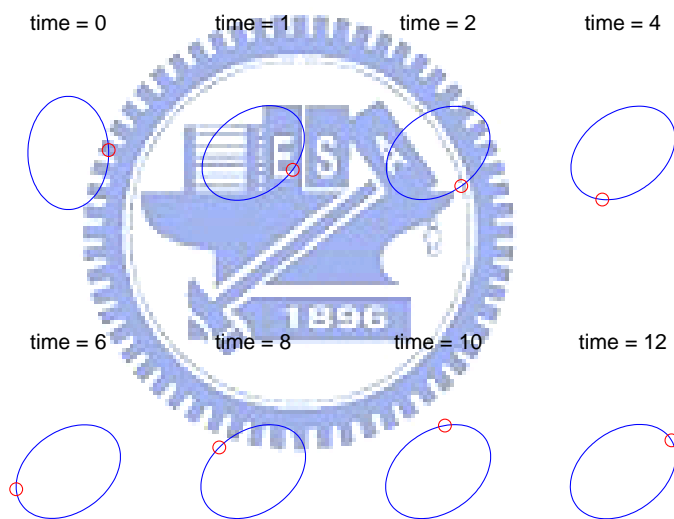


Figure 4.3: A tank-treading motion of an inextensible vesicle under a simple shear flow with the shear rate $\gamma = 1$ for $M = 128$.

Table 4.6: The mesh refinement results for the velocity (U_h, V_h) and the surface tension σ_h at $T = 0.1$.

M	$\ U_{512} - U_h\ _\infty$	order	$\ V_{512} - V_h\ _\infty$	order	$\ \sigma_{512} - \sigma_h\ _\infty$	order
64	1.60e-2	-	1.80e-2	-	2.52e-1	-
128	6.74e-3	1.24	7.45e-3	1.28	1.07e-1	1.24
256	2.23e-3	1.60	2.43e-3	1.62	3.54e-2	1.59

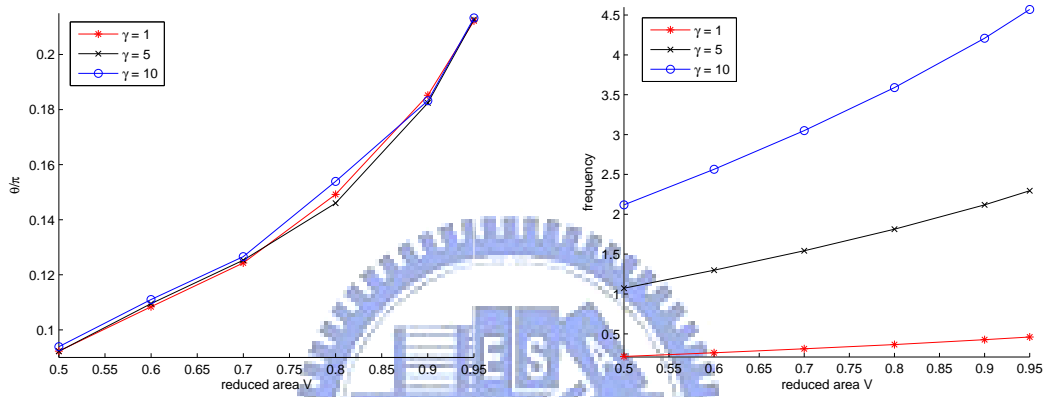


Figure 4.4: The inclination angle θ/π and the tank-treading frequency $F = \frac{2\pi}{\int_{\Gamma} \frac{1}{u \cdot \tau} ds}$ versus the reduced area V with different shear γ for $M = 128$; Left: the x-axis is the reduced area V and the y-axis is the inclination angle θ/π ; Right: the x-axis is the reduced area V and the y-axis is the tank-treading frequency $F = \frac{2\pi}{\int_{\Gamma} \frac{1}{u \cdot \tau} ds}$.

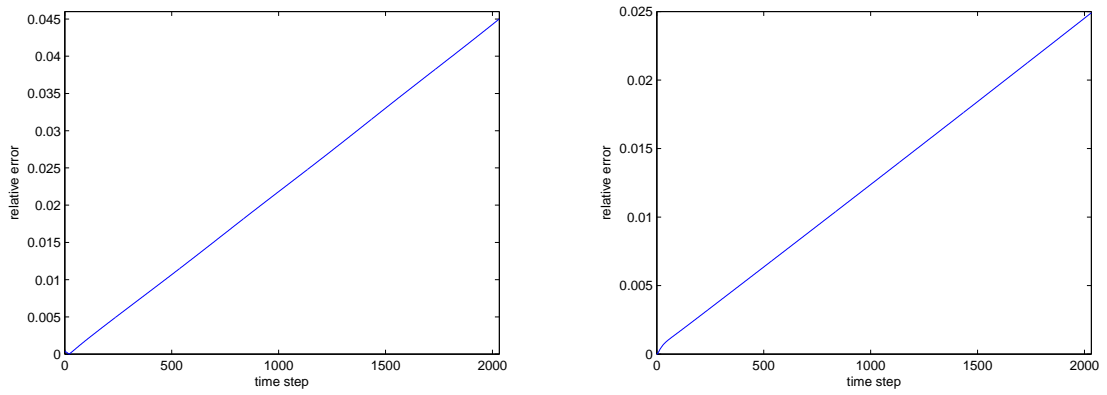


Figure 4.5: The relative error of the enclosed area A_h and the arclength L_h for $M = 128$; Left: the x-axis is the time step and the y-axis is the the relative error of enclosed area $|A_0 - A_h|/A_0$; Right: the x-axis is the time step and the y-axis is the relative error of arclength $|L_0 - L_h|/L_0$.

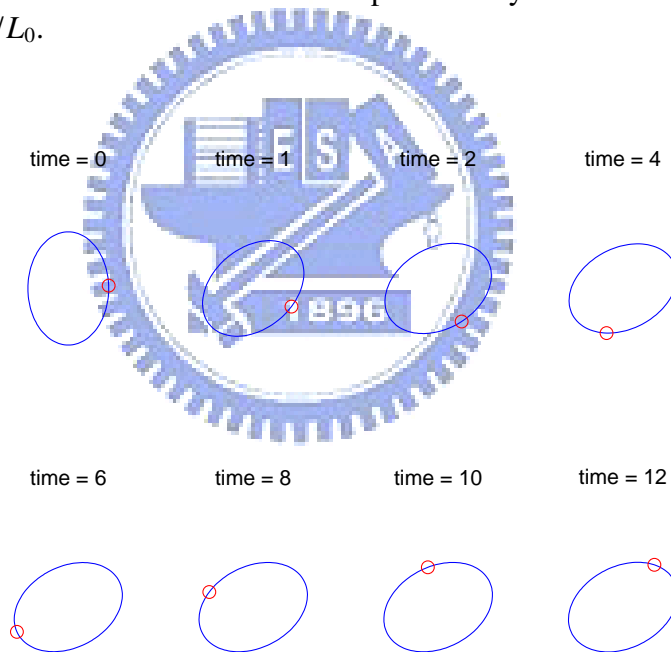


Figure 4.6: A tank-treading motion of an inextensible vesicle under a simple shear flow with the shear rate $\gamma = 1$ for $M = 128$.

Table 4.7: The mesh refinement results for the velocity (U_h, V_h) and the surface tension σ_h at $T = 0.1$.

M	$\ U_{512} - U_h\ _\infty$	order	$\ V_{512} - V_h\ _\infty$	order	$\ \sigma_{512} - \sigma_h\ _\infty$	order
64	4.76e-3	-	9.71e-3	-	1.94e-1	-
128	2.22e-3	1.10	4.03e-3	1.27	8.22e-2	1.23
256	7.72e-4	1.53	1.32e-3	1.61	2.73e-2	1.59

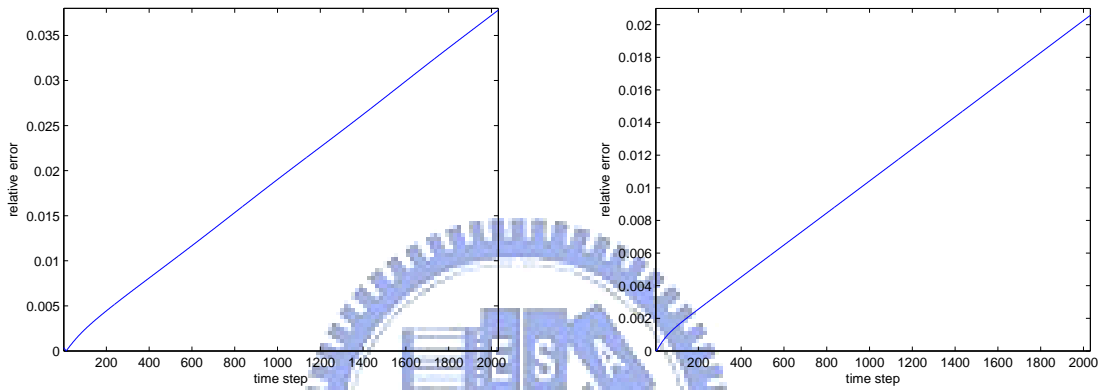


Figure 4.7: The relative error of the enclosed area A_h and the arclength L_h for $M = 128$; Left: the x-axis is the time step and the y-axis is the the relative error of enclosed area $|A_0 - A_h|/A_0$; Right: the x-axis is the time step and the y-axis is the relative error of arclength $|L_0 - L_h|/L_0$.

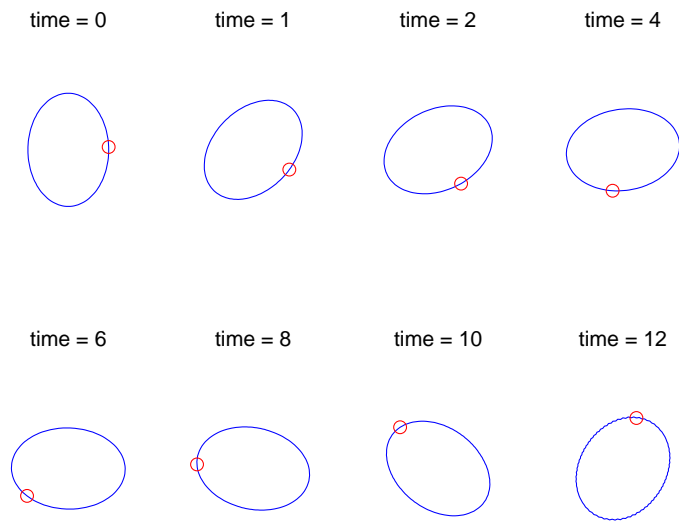


Figure 4.8: A tumbling motion of an inextensible vesicle under a simple shear flow with the shear rate $\gamma = 1$ for $M = 128$.

Table 4.8: The mesh refinement results for the velocity (U_h, V_h) and the surface tension σ_h at $T = 0.1$.

M	$\ U_{512} - U_h\ _\infty$	order	$\ V_{512} - V_h\ _\infty$	order	$\ \sigma_{512} - \sigma_h\ _\infty$	order
64	2.72e-4	-	3.95e-4	-	7.86e-2	-
128	1.07e-4	1.38	1.63e-4	1.28	3.32e-2	1.24
256	3.42e-5	1.65	5.33e-5	1.61	1.10e-2	1.59

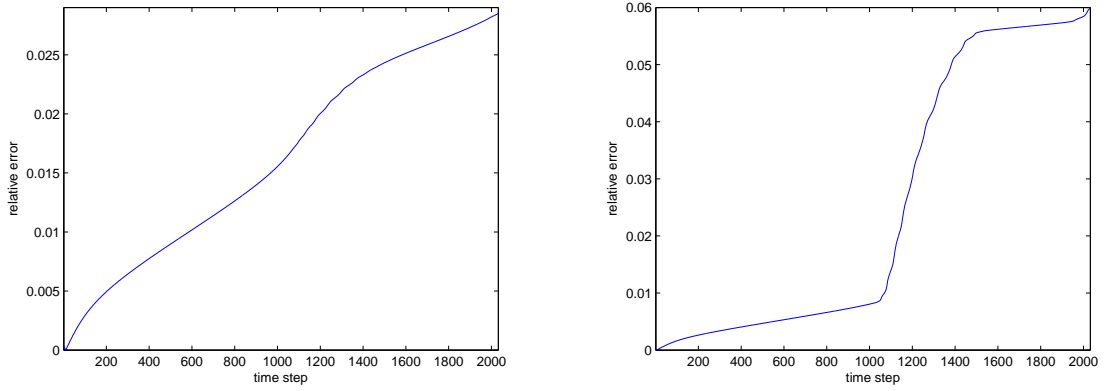


Figure 4.9: The relative error of the enclosed area A_h and the arclength L_h for $M = 128$; Left: the x-axis is the time step and the y-axis is the the relative error of enclosed area $|A_0 - A_h|/A_0$; Right: the x-axis is the time step and the y-axis is the relative error of arclength $|L_0 - L_h|/L_0$.

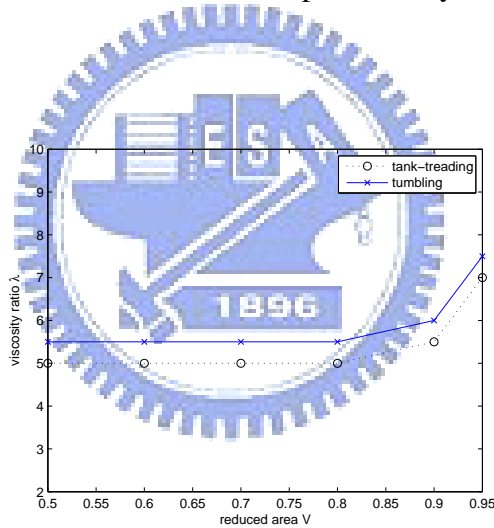


Figure 4.10: The boundary between the tank-treading motion (lower part) and the tumbling motion (upper part); Solid line: the tumbling motion; Dotted line: the tank-treading motion; The x-axis is the reduced area V ; The y-axis is the viscosity ratio λ .


5 Conclusion and future work

In this thesis, we study the boundary integral method for two dimensional incompressible Stokes flows, and analyze the singularity in the integral equations and split it into a smooth part and a singular part. The former can be treated by the trapezoidal rule and the later is cured by quadrature form with specific weights. To simulate the dynamics of an elastic interface, two numerical schemes are proposed, one is the explicit scheme

which a force in previous time step is equipped, the other is implicit so that a tension-like unknown is solved together with interfacial velocity. In numerical experiments, we first apply the method to an elliptic elastic material in a quiescent flow, and give a second-order convergence to the circular steady state. The second application is a vesicle suspended in a simple shear flow. A series of numerical studies about the tank-treading motion and the tumbling motion for a vesicle match previous works well.

Our long-term goal is to simulate the motion of multiple vesicles [13] and the dynamics of a compound vesicle [12]. In integral equation based methods, computing the interaction forces between the vesicles tends to be the dominant part of the computational cost at every time step. Simulating the dynamics of large number of interacting vesicles will be challenging. On the other hand, the transition from tank-treading to tumbling can occur in the absence of any viscosity mismatch for a compound vesicle. Moreover, a vesicle can swing if the enclosed particle is nonspherical. Accurate tracking the moving interface will require additional work.

References

- 
- [1] J. T. Beale, T. Y. Hou, J. S. Lowengrub, and M. J. Shelley, “Spatial and temporal stability issues for interfacial flows with surface tension.” *Mathl. Comput. Modelling*, Vol. 20, (1994), pp. 1-27.
 - [2] T. Hou, J. S. Lowengrub and, M. J. Shelley, “Removing the stiffness from interfacial flows with surface tension.” *Journal of Computational Physics*, Vol. 114, (1994), pp. 312-338.
 - [3] Thomas Y. Hou, and Zuoqiang Shi, “Removing the stiffness of elastic force from the immersed boundary method for the 2D Stokes equations.” *Journal of Computational Physics*, Vol. 227, (2008), pp. 9138-9169.
 - [4] Yongsam Kim, and Ming-Chih Lai, “Simulating the dynamics of inextensible vesicles by the penalty immersed boundary method.” *Journal of Computational Physics*, Vol. 229, (2010), pp. 4840-4853.
 - [5] R. Kress, “Linear integral equations.” Springer, second edition, 1999.
 - [6] Randall J. LeVeque, and Zhilin Li, “Immersed interface methods for Stokes flow with elastic boundaries or surface tension.” *SIAM Journal on Scientific Computing*, Vol. 18, (1997), pp. 709-736.
 - [7] C. Pozrikidis, “Boundary integral and singularity methods for linearized viscous flow.” Cambridge University Press, 1992.

- [8] C. Pozrikidis, "Numerical studies of cusp formation at fluid interfaces in Stokes flow." *J. Fluid. Mech.*, Vol. 357, (1998), pp. 29-57.
- [9] C. Pozrikidis, "Interfacial dynamics for Stokes flows." *Journal of Computational Physics*, Vol. 169(2), (2001), pp. 250-301.
- [10] Abtin Rahimian, Shravan Kumar Veerapaneni, and George Biros, "Dynamic simulation of locally inextensible vesicles suspended in an arbitrary two-dimensional domain, a boundary integral method." *Journal of Computational Physics*, Vol. 229, (2010), pp. 6466-6484.
- [11] Xu Sun, and Xiaofan Li, "A spectrally accurate boundary integral method for interfacial velocities in two-dimensional Stokes flow." *Commun. Comput. Phys.*, Vol. 8, (2010), pp. 933-946.
- [12] Shravan K. Veerapaneni, Y.-N. Young, Petia M. Vlahovska, and Jerzy Bławdziewicz, "Dynamics of a Compound Vesicle in Shear Flow." *Phys. Rev. Lett.*, Vol. 106, (2011).
- [13] Shravan K. Veerapaneni, Denis Gueyffier, Denis Zorin, and George Biros, "A boundary integral method for simulating the dynamics of inextensible vesicles suspended in a viscous fluid in 2D." *Journal of Computational Physics*, Vol. 228, (2009), pp. 2334-2353.

